
FUTURE PATHWAYS FOR eVTOLs: A DESIGN OPTIMIZATION PERSPECTIVE

Johannes Janning, Sophie Armanini, Urban Fasel

Department of Aeronautics, Imperial College London, United Kingdom
{johannes.janning23, s.armanini, u.fasel, }@imperial.ac.uk

ABSTRACT

The rapid development of advanced urban air mobility, particularly electric vertical take-off and landing (eVTOL) aircraft, requires interdisciplinary approaches involving the future urban air mobility ecosystem. Operational cost efficiency, regulatory aspects, sustainability, and environmental compatibility should be incorporated directly into the conceptual design of aircraft and across operational and regulatory strategies. In this work, we apply a novel multidisciplinary design optimization framework for the conceptual design of eVTOL aircraft. The framework optimizes conventional design elements of eVTOL aircraft over a generic mission and integrates a comprehensive operational cost model to directly capture economic incentives of the designed system through profit modeling for operators. We introduce a novel metric, the cross-transportation Figure of Merit (FoM), to compare the optimized eVTOL system with various competing road, rail, and air transportation modes in terms of sustainability, cost, and travel time. We investigate four objective-specific eVTOL optimization designs in a broad scenario space, mapping regulatory, technical, and operational constraints to generate a representation of potential urban air mobility stakeholder-centric design objectives. The analysis of an optimized profit-maximizing eVTOL, cost-minimizing eVTOL, sustainability-maximizing eVTOL, and a combined FoM-maximizing eVTOL design highlights significant trade-offs in the area of profitability, operational flexibility, and sustainability strategies. This underlines the importance of incorporating multiple operationally tangential disciplines into the design process, while also reflecting the diverse priorities of stakeholders such as operators, regulators, and society.

Highlights:

- Novel multidisciplinary design optimization framework for eVTOLs in UAM ecosystem.
- Critical design and cost trade-offs identified in eVTOL operations.
- Figure of Merit proposed as new benchmark for cross-modal comparison.
- Actionable strategies provided for urban air mobility stakeholders.
- Scalable eVTOL design, operations, and economic models provided.

Keywords: eVTOL; Urban Air Mobility; Multidisciplinary Design Optimization; Cost Modeling; Global Warming Potential; Sustainable Transportation System

List of Abbreviations

Abbreviation	Description
AGL	Above Ground Level
ATA	Air Transport Association
COC	Cash Operating Cost
COO	Cost of Ownership
DEP	Distributed Electric Propulsion
DOC	Direct Operating Cost
DoD	Depth of Discharge
EASA	European Union Aviation Safety Agency
EOL	End-of-Life
eVTOL	electric Vertical Take-Off and Landing
EV	Electric Vehicle
FAA	Federal Aviation Administration
FEM	Finite Element Method
FoM	Figure of Merit
GWP	Global Warming Potential
IOC	Indirect Operating Cost
MDO	Multidisciplinary Design Optimization
MTOM	Maximum Take-Off Mass
NASA	National Aeronautics and Space Administration
NCM	Nickel-Cobalt-Manganese
PAX	Passengers
SFAR	Special Federal Aviation Regulation
SLSQP	Sequential Least Squares Programming
SOC	State-of-Charge
SPL	Sound Pressure Level
TOC	Total Operating Cost
UAM	Urban Air Mobility

1 Introduction

Urban air mobility (UAM) is a vision to develop electric vertical take-off and landing aircraft (eVTOLs) to transport passengers and cargo in urban and regional networks [1]. eVTOL aircraft aim to offer fast, efficient, and sustainable transport over short to medium distances. eVTOLs will form the heart of a comprehensive ecosystem consisting of ground and airborne infrastructure, operators, and regulators. Like helicopters, eVTOLs have vertical flight capabilities, which enable them to operate in cluttered urban areas. However, they are powered by quieter and cleaner distributed electric propulsion (DEP) systems [2]. Many configurations are additionally capable of wingborne cruise flight, thus combining aerodynamic efficiency with operational versatility. eVTOLs have become technically viable only recently thanks to advances in electric systems and battery technology. However, most eVTOLs developed so far are test prototypes, and a full introduction of such vehicles in the aviation ecosystem has yet to take place. Their success will depend on meeting criteria such as low energy consumption, reduced emissions, and cost-effective operations, which are expected to promote broad public acceptance [3].

In Section 3, we explore Multidisciplinary Design Optimization (MDO) strategies for eVTOL design that balance economic profitability, ecological sustainability, travel time, and operational cost. Using a gradient-based algorithm, our framework provides an interdisciplinary platform to analyze and optimize the technological, environmental, regulatory and economic interactions in the eVTOL ecosystem. It provides a systematic platform to evaluate scenarios such as maximizing profit, minimizing cost, or reducing global warming potential to derive practical recommendations for urban air mobility stakeholders. We demonstrate this using a 70-km sizing mission, in which different regulatory and industry-specific scenarios can be analyzed, considering operational and design constraints like charging rates, rotor design and vertiport requirements. In Section 3.1.7, we introduce a new metric, the cross-transportation Figure of Merit (FoM), to balance travel time, environmental impact, and cost, and compare eVTOLs to ground-, rail-, and air-based competitors. This metric helps to provide insights to guide the development and deployment of eVTOL systems for sustainable and economically viable urban operations, considering stakeholder-preference based design decisions. Although our analysis focuses on the exemplary 70-km mission, the framework is flexible and scalable to be applied to any distance.

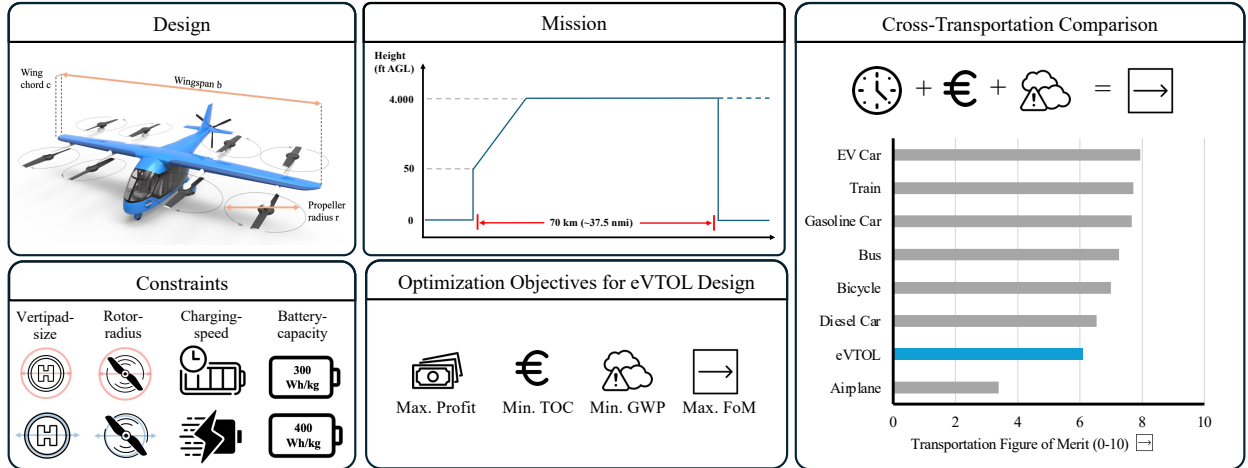


Figure 1: Framework for the conceptual eVTOL design optimization, illustrating the key geometric parameters, the mission profile, and the operational constraints. It outlines the four primary optimization objectives: maximum profit, minimum total operating cost (TOC), minimum Global Warming Potential (GWP), and maximum stakeholder-centric Figure of Merit (FoM), which are compared against conventional transportation modes (illustration adapted from [4, 5]).

2 Related work

Developing a comprehensive MDO framework for eVTOLs is crucial for addressing the complex trade-offs in UAM. Existing research primarily focuses on the optimization of aerodynamic performance, structural properties, and mission efficiency. Table 1 summarizes relevant eVTOL design and mission optimization literature, identified as related work. Several recent studies have achieved reductions in vehicle weight and improvements in energy efficiency, which are both crucial for operational feasibility [6, 7]. Despite extensive MDO research [6, 8, 7, 9, 10], however, critical aspects such as economic viability and environmental impact have been less frequently addressed. Other studies suggest potential

enhancements in mission efficiency and cost reduction but also expose notable gaps in addressing operational factors, particularly in sustainability, operations modeling, and vehicle utilization [11, 12]. Areas such as carbon footprint and battery lifecycle for eVTOL operations are rarely considered [13, 1]. Clearly, there is a need for a more integrated approach that incorporates profitability and other objectives of potential future eVTOL operators into early-stage design optimization.

Authors	Year	Objective
Kaneko et al. [6]	2023	Optimize eVTOL aerodynamics and energy efficiency for weight reduction.
Sarojini et al. [7]	2023	Optimize lift+cruise [14] weight using a geometry-centric approach.
Ruh et al. [9]	2024	Integrate physics-based models in MDO to optimize design.
Ha et al. [11]	2019	Optimize mission efficiency and profitability in eVTOL designs.
Chinthoju et al. [12]	2024	Cost optimization by varying mass, rotor radius, wing span, cruise speed.
Brown et al. [13]	2018	Design & economic optimization using geometric programming.
Kiesewetter et al. [1]	2023	Holistic UAM ecosystem state of research review & evaluation.
Silva et al. [15]	2018	Examination of lift+cruise vehicle for research & industry guidance.
Patterson et al. [14]	2018	Guideline to study UAM missions & exploration of mission requirements.
Yang et al. [16]	2021	Impact of charging strategies on battery sizing and utilization.
Kasliwal et al. [17]	2019	Physics-based analysis of VTOLs emissions vs. ground-based cars.
Schäfer et al. [2]	2019	Energy, economic and environmental implications of all-electric aircraft.
André et al. [18]	2019	Comprehensive eVTOL life-cycle assessment and design implications.
Mihara et al. [19]	2021	Cost analysis for diverse eVTOL configurations.
Lio et al. [20]	2024	Techno-economic feasibility analysis of eVTOL air taxis.
Straubinger et al. [21]	2023	Critique of UAM sustainability and equity impacts.
Straubinger et al. [22]	2022	Urban equilibrium model of UAM, CO ₂ and welfare effects.
Khavarian et al. [23]	2024	LCA of eVTOL costs and emissions in Austin network.
Fioriti et al. [24]	2024	Parametric cost and LCA models for eVTOL fleets.
Hagag et al. [25]	2023	Compare eVTOL time savings and CO ₂ vs. cars, trains, and helicopters (Paris).
Perez et al. [26]	2025	Assess economic, energy, and environmental feasibility of eVTOL commuting.
Donateo et al. [27]	2022	Compare hybrid/all-electric eVTOLs with electric road vehicles in taxi services.

Table 1: Related eVTOL design and mission optimization literature.

Table 1 summarizes related eVTOL design and mission optimization work. Brown et al. [13] employed geometric programming to optimize vehicle components and mission profiles, including noise calculations and a general cost model. However, the study provided limited detail on cost breakdowns for infrastructure, regulatory compliance, and long-term maintenance. Additionally, it did not fully address environmental costs related to energy production and battery degradation, which are essential for a comprehensive evaluation of the economic and environmental sustainability of UAM. Recent reviews have highlighted significant gaps in integrating economic models for evaluating cost-effectiveness, lifecycle costs, and environmental impacts in eVTOL design [1].

The eVTOL analysis framework developed in [15] and [14] provides insightful guidelines for eVTOL aircraft architecture and mission design that can be adapted to short- and mid-range lift and cruise eVTOL missions. Key insights on battery behavior and its implications for operational charging strategies can be drawn from [16] and [17], and critical perspectives on the interplay between economics, technology, and sustainability in fully electric aircraft are offered in [2], highlighting their interlinked nature, with [18] and [28] providing essential considerations for the environmental impacts of battery usage. A framework for standardized cost model structuring is provided in [29], and valuable input on revenue modeling is provided in [19, 20]. Finally, economic key requirements are defined for real-world operations in [30], useful for validation in eVTOL MDO.

Several studies with fixed eVTOL designs examine operations, economics, and broader societal impacts. At the network level, [23] assesses deployment in Austin, Texas, considering vertiport service areas and demand thresholds, finding that small (4-seat) vehicles can reduce emissions relative to larger types but remain cost-intensive versus ground EVs. Early-stage fleet cost and LCA models by [24] highlight maintenance, especially battery replacement, as a dominant operating cost and electricity generation as the main driver of life-cycle emissions, underscoring dependence on grid mix. From a sustainability and equity perspective, [21] argues that UAM is not inherently green, as its system-level impact may be limited, and distributional considerations are essential. Complementary LCA analyses show environmental competitiveness against cars is unlikely without low-carbon electricity and battery advances [31]. Embedding UAM within an urban spatial-equilibrium model, [22] links transport with land, labor, and goods markets and finds that welfare and emission outcomes depend on the baseline (gasoline vs. electric cars), with UAM alongside electric cars potentially worsening welfare and raising emissions. Together, these works address transportation-mode comparisons

and broader sustainability, land-use, and equity concerns, motivating the presented co-design approach that integrates vehicle design with operations, economics, and environmental impact.

Beyond eVTOL-specific MDO, earlier transport research has introduced cross-modal performance metrics to compare the efficiency of different modes of transportation. The Gabrielli–von Kármán diagram established fundamental limits of transport performance across speed regimes [32], and subsequent updates have extended this framework with modern data and improved figures of merit [33, 34]. Other studies have focused on eco-efficiency indicators for urban transport [35, 36], balancing energy use, emissions, and service value. Case studies have analyzed eVTOLs against competing modes in powertrain-level comparisons [27], and in location-specific contexts such as Paris [25] and Chicago [26]. These works provide valuable insights into cross-modal trade-offs and high-level transport efficiency, urban eco-efficiency metrics, and location-specific case studies. A generalizable and integrated metric for systematically benchmarking eVTOLs against the broader transport system is still missing, motivating the cross-transportation Figure of Merit introduced in this work.

3 Methodology

3.1 Multidisciplinary Design Optimization

The presented eVTOL aircraft design framework uses a Sequential Least Squares Programming (SLSQP) algorithm as a gradient-based optimizer to solve a set of single-objective, multidisciplinary design optimizations. A multi-start strategy is applied, where the algorithm is run from multiple random initial points, to mitigate sensitivity to local minima. The design variables are normalized to the $[0, 1]$ range to improve numerical stability [8]. Table 2 summarizes the optimization problem statement for the four independent and separately run single-objective optimizations of the Figure of Merit, total operation cost, operating profit, and operational global warming potential. A detailed description and remarks on the selection of the optimization approach can be found in Section 8 of the supplementary materials. Figure 2 illustrates the extended design structure matrix [37] outlining the model integration. The optimization feeds into a system model including mass estimation, environmental impact assessment, cost modeling, and the scoring-based Figure of Merit. Model details are provided in the following sections and supplementary material.

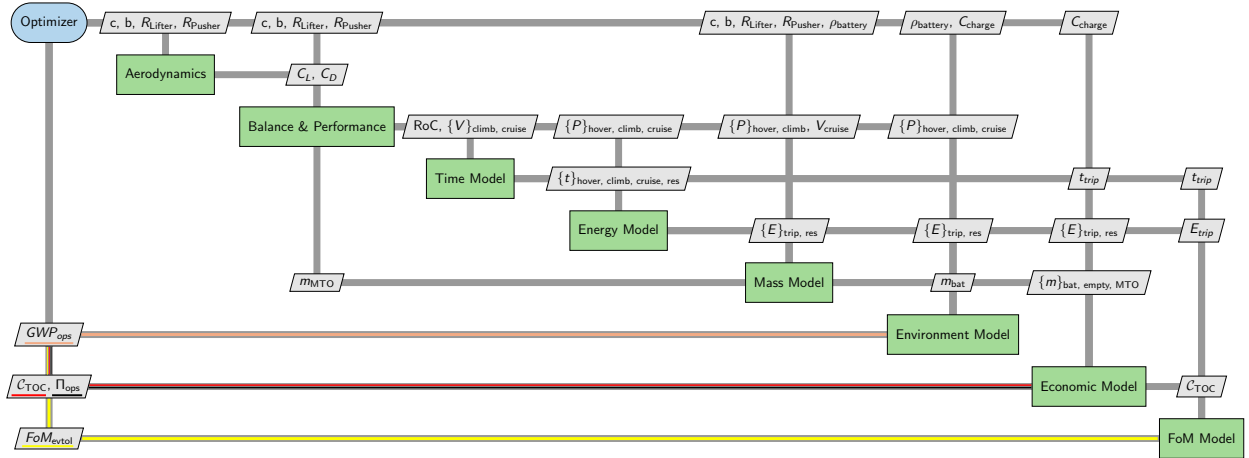


Figure 2: Extended Design Structure Matrix for single-objective optimization: FoM_{evtol} , yellow line; Total Operating Cost C_{TOC} , red line; Operating Profit Π_{ops} , black line; Operational Global Warming Potential GWP_{ops} , light brown.

The design variables of Table 2 are bounded to reflect practical design limits and current and near-term feasibility of eVTOL aircraft systems. The wingspan is bounded as $b \in [6, 15]$ m, the wing chord as $c \in [1, 2.5]$ m, the cruise rotor radius as $R_{cruise} \in [0.5, 2.5]$ m, and the hover rotor radius as $R_{hover} \in [0.5, 2.0]$ m. Battery energy density is bound to $\rho_{bat} \in [200, 400]$ Wh/kg, and the charging rate to $C_{charge} \in [1C, 4C]$. A brief classification of the optimization variable bounds is provided in Section 3.2. A detailed derivation of the wing and vertiport geometry constraints can be found in Section 7 of the supplementary material.

3.1.1 Mass Estimation

The maximum take-off mass (M_{MTO}) consists of the payload mass $M_{payload}$, the eVTOL empty mass M_{empty} , and the battery mass $M_{battery}$:

		Function/Variable	Description
Objective Type (in separate SO runs)	objective	max. FoM_{evtol}	Transportation Figure of Merit (0–10)
		min. C_{TOC}	Total operation cost per mission (€)
		max. Π_{ops}	Operating profit (€)
		min. $GW P_{\text{Ops}}$	Operational global warming potential (kg CO ₂ e)
by varying	design vars	R_{lifter}	Lifting rotor radius (m)
		R_{pusher}	Pusher rotor radius (m)
		c	Aircraft wing chord (m)
		b	Aircraft wing span (m)
		ρ_{battery}	Battery energy density (Wh/kg)
		C_{charge}	Battery charging rate (C-rate) (1/h)
subject to	geometry	$b \geq 2(3R_{\text{hover}} + 2d + r_{fus})$	Wing span must fit hover rotor and fuselage layout (m)
		$15 \geq 2(4R_{\text{hover}} + 2d + r_{fus})$	Total layout must fit average vertiport width (m) [38]
	regulation	$M_{\text{MTOM}} \leq 5,700$	Max. take-off mass limit (kg) [39]
	noise	$SPL_{\text{hover}} \leq 77$	Max. noise level at 250 ft (dB(A)) [30]
	rotor speed	$RPM_i \leq 3,000$	Max. propeller rotational speed per phase (rpm)
	airspace	$V_i \leq 129$	Speed limit for climb and cruise phases (m/s) [39]

Table 2: Formulation of the single-objective optimization (SO) problem, repeated for four distinct objectives. d is the required rotor-to-rotor clearance, r_{fus} is the fuselage radius, and i indexes the flight phases: hover, climb, and cruise.

$$M_{\text{MTOM}} = M_{\text{payload}} + M_{\text{empty}} + M_{\text{battery}} \leq \text{Limit}_{\text{certification}}. \quad (1)$$

According to the European Union Aviation Safety Agency’s (EASA) latest certification specifications for eVTOL, the maximum certifiable mass is limited to $\text{Limit}_{\text{certification}} = 5,700$ kg [40]. M_{battery} is considered separately from M_{empty} due to the significant impact the batteries have on the MTOM, and as batteries can be exchanged flexibly if necessary. A detailed description of the mass models is provided in Section 2 of the supplementary material. M_{battery} is calculated using the following equation taking into account the design mission energy requirements and battery energy density ρ_{bat} in Wh/kg, with a factor of 0.64 to account for unusable battery energy, introduced in Section 3.1.3:

$$M_{\text{battery}} = \frac{E_{\text{useable}}}{e_{\text{usable}}} = \frac{E_{\text{trip}} + E_{\text{res}}}{0.64 \cdot \rho_{\text{bat}}}. \quad (2)$$

The empty mass M_{empty} is defined as:

$$M_{\text{empty}} = M_{\text{wing}} + M_{\text{gear}} + M_{\text{rotor}} + M_{\text{motor}} + M_{\text{fuselage}} + M_{\text{systems}} + M_{\text{furnish}} + M_{\text{crew}}, \quad (3)$$

where M_{wing} , M_{fuselage} , M_{gear} , M_{systems} , and M_{furnish} are estimated according to Raymer [41] and Nicolai [42]. These regression models serve as statistical first-order estimates based on vehicle geometry derived from conventional general aviation aircraft, and may not capture eVTOL-specific structural requirements such as vertical crash loads or extensive composite use. They are applied as conceptual approximations, with higher-fidelity FEM analyses for diverse load cases identified as a potential extension in future work. M_{furnish} is the predicted weight of furnishings, non-structural components that are necessary to equip the aircraft for the operation and comfort of the crew and passengers. Crew mass M_{crew} is based on average masses for single pilot operation [43]. The rotor mass M_{rotor} is computed by a radius-based regression adopted from [6], intended for early conceptual design. The motor mass M_{motor} is modeled by a power-based empirical regression [44], including a power sizing margin factor of $s = 1.5$. This factor scales the required mission power to the available installed power per propulsor to ensure that $P_{\text{available}} \geq P_{\text{required}}$ across all design-mission segments. The modeled M_{rotor} and M_{motor} provide statistical first-order estimates and do not capture detailed design requirements. Higher-fidelity methods may be applied in future work to refine these estimates. M_{payload} accounts for average mass of passenger M_{pax} and luggage per passenger M_{lug} [43], calculated as:

$$M_{\text{payload}} = (M_{\text{pax}} + M_{\text{lug}}) \cdot n_{\text{seats}} \cdot LF. \quad (4)$$

In this work, we consider a fully loaded 4-seater eVTOL (excl. pilot) as sizing requirement, resulting in a fixed payload of 392.8 kg.

3.1.2 Aerodynamic Model

We use a simplified aerodynamic lift and drag coefficient model of the eVTOL wing [6, 45], and use airfoil data for a NACA2412 airfoil at $Re = 4 \times 10^6$ [46]. A detailed description of the aerodynamic models is provided in Section 3 of the supplementary material. While this simplified model is convenient for fast optimization and allows for the consideration of multiple subsystems, the same framework can be extended to more complex models in future work. The model for the lift coefficient C_L assumes a linear pre-stall lift curve, using the finite-wing lift coefficient:

$$C_L = \frac{\alpha_{airfoil}}{1 + \frac{\alpha_{airfoil}}{\pi \cdot AR \cdot e}} \cdot \alpha + C_{L_0}, \quad (5)$$

where $\alpha_{airfoil}$ is the airfoil lift-curve slope, AR is the wing aspect ratio, and e is the Oswald efficiency factor. Total lift is then calculated as:

$$L = \frac{1}{2} \cdot \rho \cdot V^2 \cdot S \cdot C_L = \frac{1}{2} \cdot \rho \cdot V^2 \cdot S \cdot \left(\frac{\alpha_{airfoil}}{1 + \frac{\alpha_{airfoil}}{\pi \cdot AR \cdot e}} \cdot \alpha + C_{L_0} \right). \quad (6)$$

The model for the drag coefficient C_D is based on lifting line theory [45], and assumes that the finite-wing drag coefficient is composed of induced drag C_{D_i} and parasite drag $C_{D_{min}} = 0.0397$ [6]:

$$C_D = C_{D_{min}} + C_{D_i} = C_{D_{min}} + \frac{C_L^2}{\pi \cdot AR \cdot e}. \quad (7)$$

The total drag is then calculated as:

$$D = \frac{1}{2} \cdot \rho \cdot V^2 \cdot S \cdot C_D = \frac{1}{2} \cdot \rho \cdot V^2 \cdot S \cdot \left(0.0397 + \frac{C_L^2}{\pi \cdot AR \cdot e} \right). \quad (8)$$

3.1.3 Power & Energy Model

The models presented in this subsection are fully derived in Chapter 4 of the supplementary material. The power requirements for hover P_{hover} , climb P_{climb} , and cruise P_{cruise} are computed using momentum theory derived from force balance equilibrium [47, 48], considering thrust requirements of the respective flight phase T_{req} , rotor diameter R , max. take-off mass, air density ρ , induced velocity v_i , climb angle θ (assuming zero wind, thus $\theta = \alpha$) and propulsion efficiency η [13, 16]. The system efficiencies are described in Section 4.1 of the supplementary material. Due to the conceptual nature of our work, we assume no wing incidence and zero wind effects. Therefore, we consider angle of attack (α), pitch angle (θ), and flight path angle (γ) to be equivalent ($\alpha = \theta = \gamma$). The time requirement for each flight phase is calculated considering the speeds for climb V_{climb} and cruise V_{cruise} , derived from force balance equilibrium of the related flight phase [48]. Thrust angle α_t and pitch angle θ are assumed to be equivalent to the angle of attack during cruise, α_{cruise} , and climb α_{climb} , respectively. The hover time is assumed to be fixed at a total of 60 seconds [30]. This results in the distance-bridging energy requirement for the sizing mission:

$$E_{trip} = \sum_i P_i \cdot t_i = P_{hover} \cdot t_{hover} + P_{climb} \cdot t_{climb} + P_{cruise} \cdot t_{cruise}. \quad (9)$$

The maximum usable trip energy in the battery results from the consideration of 30min reserve in cruise power conditions, and unusable energy in the battery. The unusable energy is derived from 10% ceiling and 10% floor state-of-charge (SOC), and the assumption that the battery is operated in its end-of-life (EOL) state, defined by a 20% degradation [16], resulting in specific battery energy at EOL:

$$e_{BAT_{EOL}} = 0.8 \cdot \rho_{bat}. \quad (10)$$

For a given battery energy density ρ_{bat} in Wh/kg, the usable specific energy available for the sizing mission is:

$$e_{usable} = 0.8 \cdot e_{BAT_{EOL}} = 0.64 \cdot \rho_{bat} = e_{trip_{sizing}} + e_{reserve}. \quad (11)$$

3.1.4 Rotor Acoustic Model

The noise emitted by eVTOL is seen as one of the main challenges for social acceptance and thus the general success of urban air mobility [3]. For simplicity and clarity, tonal rotor noise is modeled for hover flight, while broadband noise is modeled for climb and cruise phases. Combined contributions are not considered. The Sound Pressure Level (SPL) in hover, climb, and cruise are considered as constraints in the optimization, as outlined in Table 2. We assume an allowable SPL of 77 dB(A) at an observer distance of 250ft, which is 10dB(A) lower and perceived half as loud as a typical small four-seat helicopter [30]. To compute the tonal SPL for hovering rotors, we apply the Gutin-Deming model [49, 50, 51]. The equations for these models are detailed in Section 7.1 of the supplementary material, including all input variables and constants.

The broadband sound pressure level is based on the model by Schlegel, King, and Mull (SKM) [52], accounting for several key factors influencing noise during the climb and cruise phases. The SPL is primarily determined by a constant, the propeller's effective area, and the blade tip velocity. The model also includes corrections for the propeller's lift coefficient and the observer's distance, which change between the climb (250 ft) and cruise (4000 ft) phases.

While the SKM model provides a practical estimation of broadband rotor SPL based on semi-empirical scaling, its accuracy is limited by simplified aerodynamic assumptions and empirical calibration, and should be complemented by higher-fidelity methods in later design stages. In addition, it should be noted that SPL alone is not entirely representative of public noise exposure, as individual annoyance is also dependent on the physiological perception of loudness. This is quantified by the Day Night Level (DNL) [30], and should be monitored and assessed individually at the vertiport sites during operation. The cumulative noise impact of eVTOL fleet operations should be considered in future work, as large scale deployment may require lower SPL targets such as 67dB at 250ft [30]. This more stringent constraint is not considered in the presented study to avoid over-constraining the model. Further modeling details and assumptions are given in Section 7.1 of the supplementary material.

3.1.5 Economic Model

The presented economic model considers a hierarchical cost model structure based on Air Transport Association (ATA) [29] and a revenue model inspired by UberElevate [30, 53]. The operations are based on Uber's assumptions of 280 annual working days per eVTOL with an 8-hour operating window. While not modeled in this work, real-world operation windows need to be evaluated more closely in future studies in light of regional weather conditions and weather statistics, as it can be assumed that eVTOLs will initially operate exclusively under visual flight rules, which excludes operations in hazy, low visibility weather conditions [1].

A detailed derivation of the cost models and underlying assumptions is provided in Section 5.2 of the supplementary material. Total operating costs per flight (TOC) are defined as the sum of cash operating costs (COC), cost of ownership (COO) and indirect operating costs (IOC). The sum of COC and COO is defined as direct operating costs (DOC):

$$TOC = COC + COO + IOC, \quad (12)$$

with IOC being a fixed percentage of 22% of DOC [54]. COC are directly related to flight operations taking into account energy cost C_E , salary-based crew cost C_C , mass-based navigation/ATC cost C_N and maintenance cost C_M . C_M is the sum of wrap-rated maintenance cost C_{wrm} according to [13] and battery replacement cost C_{MB} :

$$COC = C_E + C_C + C_N + C_{wrm} + C_{MB}. \quad (13)$$

COO accounts for insurance C_{ins} , as 6% of COC [19], and capital expenditure, as annual depreciation cost C_{dep} [55]:

$$COO = C_{ins} + C_{dep}. \quad (14)$$

The profit model is based on the revenue calculation using a fixed kilometer-based fee [30]. This fee is based on the mileage rate for trips during the day of London cabs [56] as a first estimation. Future extensions of this model should consider demand-based revenue modeling to capture more realistic revenue management strategies. The accumulated annual profit over the number of flight cycles FC_a is then expressed as:

$$Profit_{flight} = FC_a \cdot (Rev - TOC) = FC_a \cdot (fare \cdot d_{trip} - TOC). \quad (15)$$

While the cost model components are adapted from established frameworks, their novelty in this study lies in their integration with environmental (GWP) and transportation preference (FoM) models within a unified multidisciplinary optimization framework. This enables a consistent assessment of economic, environmental, and operational trade-offs in conceptual eVTOL design.

3.1.6 Global Warming Potential Model

The global warming potential (GWP) considered in this work is derived from the GWP impact of electricity generation and the life-cycle emissions of the batteries used. The GWP impact of the energy consumed is based on the International Energy Agency (IEA) data for Germany [57, 58, 59], assumed as 0.38 kg CO_2e per kWh. However, our framework also allows for the application of the energy production GWP of a large number of other regions. The operational energy-based GWP per flight cycle is calculated as:

$$GWP_{\text{energy,cycle}} = E_{\text{trip}} \cdot GWP_{\text{energy}}, \quad (16)$$

where E_{trip} is the mission energy consumption [kWh] and GWP_{energy} is the specific GWP of electricity production [kg CO_2e /kWh]. The output $GWP_{\text{energy,cycle}}$ is given in [kg CO_2e].

A simple empirical battery degradation model is used, which is described in Section 6 of the supplementary material. We model the life-cycle of a lithium-ion battery based on the depth of discharge, battery charging rate, and flight phase average battery discharge rate. If we relate the life-cycle of the battery to the operational charging cycles, we can estimate the number of annual required batteries.

$$N_{\text{bat,year}} = \frac{N_{\text{wd}} \cdot T_D}{N_{\text{cycles}} \cdot t_{\text{trip}} \cdot DH}, \quad (17)$$

where N_{cycles} is the available discharge cycle life of the battery, N_{wd} the number of working days per year, T_D the daily operating time, t_{trip} the average trip time, and DH the time efficiency ratio defined as $\frac{t_{\text{turnaround}}}{t_{\text{trip}}} + 1$ (see Section 3.2). This first-order estimate does not account for battery swapping strategies or partial-cycle utilization.

We assume a life-cycle GWP of 124.5 kg CO_2e per kWh battery capacity [28], based on Nickel-Cobalt-Manganese (NCM) lithium-ion batteries, which are widely used in electric vehicles (EVs) and increasingly in aviation due to their high energy density and favorable weight-to-performance ratio [1]. The GWP of the battery accounts for raw material extraction and processing, battery manufacturing, transportation, and end-of-life treatment [18]. The battery life-cycle GWP per flight cycle is calculated as:

$$GWP_{\text{battery,cycle}} = \frac{N_{\text{bat,year}}}{FC_a} \cdot GWP_{\text{battery}} \cdot E_{\text{battery,design}}, \quad (18)$$

where GWP_{battery} is the specific GWP of battery production [kg CO_2e /kWh], $E_{\text{battery,design}}$ the design battery capacity [kWh], $N_{\text{bat,year}}$ the number of batteries required annually, and FC_a the annual number of flight cycles. Further details on the operational metrics are provided in Section 5 of the supplementary material. The total annual operational GWP is calculated as:

$$GWP_{\text{annual}} = FC_a \cdot (GWP_{\text{operational,cycle}} + GWP_{\text{battery,cycle}}) \quad (19)$$

It should be noted that the presented GWP assessment does not include the full life-cycle of the eVTOL aircraft itself, such as structural components, manufacturing, maintenance, or end-of-life disposal. Nonetheless, the presented framework and analysis can be expanded to include this aspect in future work, e.g. based on the work in [18].

3.1.7 Transportation Figure of Merit

We introduce the Transportation Figure of Merit (FoM) to analyze and compare the attractiveness of eVTOL versus other transportation alternatives, and to examine when and why a mode of transportation can be considered competitive in relation to specified objectives. This metric is a stakeholder-centric index that aims to quantify the utility of each transport option (see Table 3) by time, cost, and CO_2e emissions in a single rating. This allows for comparing the designed eVTOL aircraft with alternative means of transportation over equivalent travel distance. In the context of our analysis, we refer to the sizing mission of 70 km (see Figure 3). The sizing mission distance is the straight-line distance traveled by the eVTOL. To account for real traffic patterns, we use the mode-specific circuitry factor to compute the true distance traveled [30], the ratio between the actual distance traveled and the straight-line path. This takes into account detours caused by road networks, flight routes, or rail topology to provide a more realistic travel estimate.

For each transport mode j , the values for cost, CO_2e , and travel time ($x_{j,k}$ for $k \in \{1 = \text{cost}, 2 = CO_2, 3 = \text{time}\}$) are obtained by applying the base metrics presented in Table 3 to the defined trip distance. The three criteria ($k \in 1, 2, 3$) were selected due to their availability, quantifiability, and relevance in both stakeholder-centric and policy-related transport assessment. Metrics such as reliability, accessibility, availability, safety, and travel demand (e.g., mode-specific trip density or service coverage) also provide valuable insights, but are not included in our analysis and should be integrated into future extensions of this framework. Each criterion is normalized into a rating between 0 and 10 using Eq. (20), where the transport mode with the best performing metric receives a score of 10, and the worst performing

Vehicle (Load factor), j	\emptyset -V (km/h)	\emptyset Cost/skm	\emptyset CO_2e /skm	Circuitry (-)	Source
Gasoline Car (100%)	85	0.023	0.031	1.3	[60, 61, 62]
Gasoline Car (26%)	85	0.090	0.120	1.3	
Gasoline Car (20%)	85	0.117	0.157	1.3	
Diesel Car (100%)	85	0.017	0.026	1.3	[63, 64, 65, 66]
Diesel Car (26%)	85	0.064	0.099	1.3	
Diesel Car (20%)	85	0.083	0.128	1.3	
Electric Car (100%)	85	0.021	0.013	1.3	[67, 68, 69]
Electric Car (26%)	85	0.081	0.050	1.3	
Electric Car (20%)	85	0.105	0.065	1.3	
Public Bus (diesel) (100%)	64	0.06	0.013	1.6	[70, 64, 66, 65]
Public Bus (diesel) (60%)	64	0.104	0.022	1.6	
Public Train (electric) (100%)	99	0.2	0.007	1.2	[71, 72]
Public Train (electric) (50%)	99	0.402	0.012	1.2	
Airplane, jet (100%)	74 ^(*)	0.46	0.198	1.05	[73, 74]
Airplane, jet (79.6%)	74 ^(*)	0.579	0.249	1.05	
Bicycle (100%)	18.8	-0.491 ^(**)	0.0	1.28	[75, 76]

Table 3: Transportation performance metrics for average travel velocity, cost, emission expenditure, and circuitry of conventional transportation modes, used as baseline for the Transportation Figure of Merit (FoM) comparison. Sources apply to all load factor scenarios within each vehicle class. ^(*) Accounts for an additional two hours for security and boarding procedures as recommended by airlines. ^(**) Negative cost as considers personal health impact (skm = seat-kilometer).

one is rated 0. All other results are interpolated proportionally in between. Let $x_{j,k}$ denote the value of criterion k for vehicle j . The normalized rating $R_{j,k}$ is computed as:

$$R_{j,k} = \frac{(x_{j,k} - X_{\min}^{(k)}) - 10 \cdot (x_{j,k} - X_{\max}^{(k)})}{X_{\max}^{(k)} - X_{\min}^{(k)}}, \quad (20)$$

where $X_{\min}^{(k)} = \min_j x_{j,k}$ and $X_{\max}^{(k)} = \max_j x_{j,k}$ are the minimum and maximum values of criterion k across all vehicles. The overall FoM is subsequently calculated by weighting each rating to quantify the combined utility, with $\sum_{k=1}^3 w_k = 1$. For vehicle j , with the normalized rating $R_{j,k}$ with respect to criterion k , the FoM defined as:

$$\text{FoM}_j = \sum_{k=1}^3 w_k \cdot R_{j,k} \quad (21)$$

For our analysis and the absence of real-world stakeholder preferences, we assume a stakeholder who weights each criterion k equally, to provide a transparent and balanced consideration within the presented work as $w_k = \frac{1}{3} \forall k$. Future studies may investigate a variation in the weightings to explore the behavior of stakeholders at particular cost, time, or CO_2e sensitivity in more depth to reflect real-world preferences.

3.2 Optimization bounds

The design variables defined in Table 2 in Section 3.1 are bounded to reflect the current feasibility and medium-term technological potential of eVTOL systems. As described in Table 4, the lower limits correspond to restrictive assumptions based on existing technology and regulatory constraints, while the upper limits represent projected assumptions consistent with expected advances, especially in battery technology, and extended design capabilities. The interpretations of the boundaries are used in the further analysis to derive regulatory and operational conditions for the optimized design and determine appropriate recommendations.

The charging C -rate directly influences the modeled turnaround time in eVTOL operations. For simplicity, the leg time t_{leg} is expressed as the sum of flight time and turnaround time, where the flight time is a function of the vehicle velocity in different flight phases, the trip distance, and the hover duration:

	Lower bound	Upper bound
Wing span b	6 m: Compact wing suitable for highly constrained urban settings.	15 m: Reflects urban space limitations and integration challenges with existing urban infrastructure [77].
Wing chord c	1.0 m: Narrow chord consistent with compact, lightweight designs.	2.5 m: Wide chord accommodates structural and aerodynamic performance at higher loads.
Rotor radius R	0.5 m: Aligns with industry benchmarks and UAM constraints, offering a realistic framework for current designs (industry comparison in supplementary material Section 7).	2.5 m: Allows exploration of scenarios with fewer spatial and noise constraints, suitable for suburban or rural eVTOL applications.
Battery density ρ_{bat}	200 Wh/kg: Represents the current state of lithium-ion technology, providing a conservative and realistic baseline for today's eVTOL designs.	400 Wh/kg: Anticipates future battery advancements, aligning with industry targets and enabling extended range and performance scenarios [1].
Charging rate C_{charge}	1C: Assumes slow charging, offering a conservative scenario, especially in urban areas with limited fast-charging.	4C: Supports rapid charging, enabling faster service cycles as intended by various UAM providers [1].

Table 4: Optimization bounds: lower bounds represent conservative, near-term feasibility; upper bounds reflect forward-looking technological and infrastructural assumptions.

$$t_{\text{flight}} = f(V_i, D_{\text{trip}}, t_{\text{hover}}), \quad i \in \{\text{climb}, \text{cruise}\}, \quad (22)$$

and the turnaround time is modeled as a function of the charging rate and the depth-of-discharge (DoD), taking into account the battery charging time:

$$t_{\text{turnaround}} = f(C_{\text{charge}}, \text{DoD}). \quad (23)$$

Boarding and disembarking times are not taken into account due to the relatively low passenger throughput per aircraft compared to conventional civil aviation ground procedures. A more detailed modeling of the turnaround process should be considered in future work. A more detailed formulation of the underlying models is provided in Section 5.1 of the supplementary material.

3.3 Sizing mission

This study adopts the sizing mission profile proposed by National Aeronautics and Space Administration (NASA) [14], which is characterized by a 37.5 nautical mile (~ 70 km) travel distance and a cruise altitude of 4,000ft above ground level (AGL), shown in Figure 3. This widely accepted mission profile aligns with established research ([15], [14]), enhancing the comparability of the presented findings within academic and industry contexts.

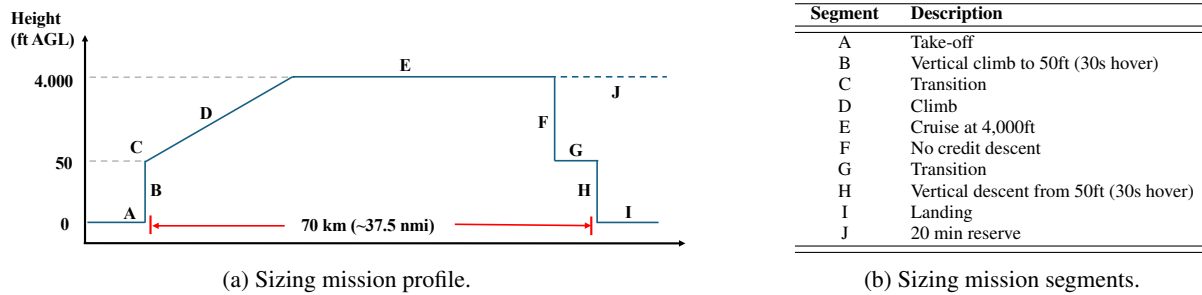


Figure 3: Sizing mission: (a) profile and (b) segments.

The use of these parameters reflects realistic operational conditions for urban and regional air mobility, including typical city-to-city or intra-urban flights. By incorporating key operational phases such as vertical climb, cruise climb and

cruise, this mission profile provides comprehensive insights into eVTOL performance, including energy consumption and battery requirements. The modeling of the transition phase is not included in this study to reduce complexity, and should be addressed in future high-fidelity analyses to capture transient aerodynamic effects, control requirements, and potential impacts on energy consumption and noise generation. Additionally, a 20-minute cruise reserve is applied in accordance with the Federal Aviation Administration (FAA) Special Federal Aviation Regulation (SFAR) requirements [78].

3.4 Analysis workflow

The presented analysis builds on the MDO framework introduced in Section 3.1. The four objectives are optimized independently in separate single-objective runs, subject to a constant set of defined design variables, bounds, and constraints: (1) maximum annual profit, (2) minimum operating cost per trip, (3) minimum annual global warming potential (GWP), and (4) maximum transportation figure of merit (FoM). This setup ensures comparability across objectives while allowing each optimization to highlight a distinct design priority. The outcome of each single-objective optimization is an optimal conceptual eVTOL configuration and operations setup, tailored to its specific design priority. In Section 4, these designs are first discussed individually to identify how cost, profit, emissions, or user utility shape the resulting aircraft geometry, performance, and operations. Subsequently, the results are compared across objectives to expose trade-offs between economic, environmental, and operational considerations. In Section 5, the obtained designs are benchmarked against external industry requirements [30, 53]. By contrasting the resulting optima, we gain insights into potential pathways toward balanced trade-off designs that reconcile competing stakeholder objectives and support the alignment of technical capabilities with anticipated operational environments.

4 Results

4.1 Profit-maximized eVTOL design

The profit-maximizing eVTOL design, illustrated in Figure 4, was obtained after 8 iterations and 58 function evaluations, with a runtime of 1.36 seconds, and achieves an annual operating profit of €1.49 million. The optimizer converged to a medium wing span of 10.9 m with a slender chord of approximately 1.0 m, a cruise propeller radius of 2.50 m, and moderate hover rotors of 1.64 m, thus remaining within the 15 m vertiport diameter constraint while balancing aerodynamic efficiency and mass. This configuration enables a cruise speed of 81 m/s at a lift-to-drag ratio of 10.9, leading to a 16.1-minute trip time. The maximum take-off mass is 2,379 kg with an empty-mass fraction of 0.495 and a relatively high battery fraction of 0.34, still within the range for eVTOL designs [1]. At a pack-level energy density of 290 Wh/kg, the required design capacity of 234.7 kWh translates into a battery mass of 809 kg, which in turn reflects the model formulation that directly couples aircraft mass to cruise velocity. It should be noted that future extension of this study should allow explicit speed management as a design parameter to better align battery sizing with operational efficiency. With an upper-limit charging rate of 4C, turnaround is performed in 4.6 minutes, resulting in a block time of 21 minutes per flight, including charging, which allows more than 6,000 annual cycles and about 1,600 annual flight hours. Profitability is determined by the combined effect of per-flight margin and annual vehicle utilization, which are both maximized by the selected geometry. A high-aspect-ratio wing with a large cruise propeller reduces power demand in climb and cruise, lowering trip energy to 72.6 kWh, while the short airborne segment due to fast climb and cruise combined with moderate battery depth-of-discharge shortens both trip and charging times. This combination yields approximately 23 flights per day, which is only feasible under the assumption of sufficient demand, a factor that should be examined in future demand–supply modeling to extend this work. Although battery replacements account for more than a quarter of the total operating cost of €129 per flight, the high number of daily cycles enabled by short block times more than compensates for this penalty, making annual utilization the dominant driver of profit. Energy cost per trip is €7.02 (5% of TOC), crew cost is €7.81 (6% of TOC), and time-based maintenance amounts to €8.83 (7% of TOC). Navigation charges are €21.75 (17% of TOC) and ownership costs €27.08 (21% of TOC), both directly scaling with MTOM. The major penalty of this design arises from the battery management, allowing fast charging times at the cost of accelerated cycle wear, reducing lifetime to about 801 charging cycles and resulting in 7.5 battery replacements per year. With a unit pack cost of €26,992 (115 €/kWh, [19]), this corresponds to €33.7 per flight or 26% of TOC. SPL and environmental performance reveal further trade-offs as the design converges to the upper noise constraint in hover, a consequence of the relatively high MTOM and modest hover rotor radius. While still compliant, the very high frequency of operations implied by this design would amplify community noise exposure, which is not yet accounted for in the present study and should be considered in future operational assessments. From an environmental impact perspective, the design produces 386 tons of CO₂e per year, corresponding to 0.23 kg CO₂e per available seat-kilometer, of which 43% is attributed to electricity generation for battery usage and 57% to battery replacement impact. This translates to 90 gasoline-powered passenger vehicles or 341 electric-powered passenger vehicles driven for one year [79]. Although eVTOL aircraft emit no direct operating emissions, the impact of energy production for charging and

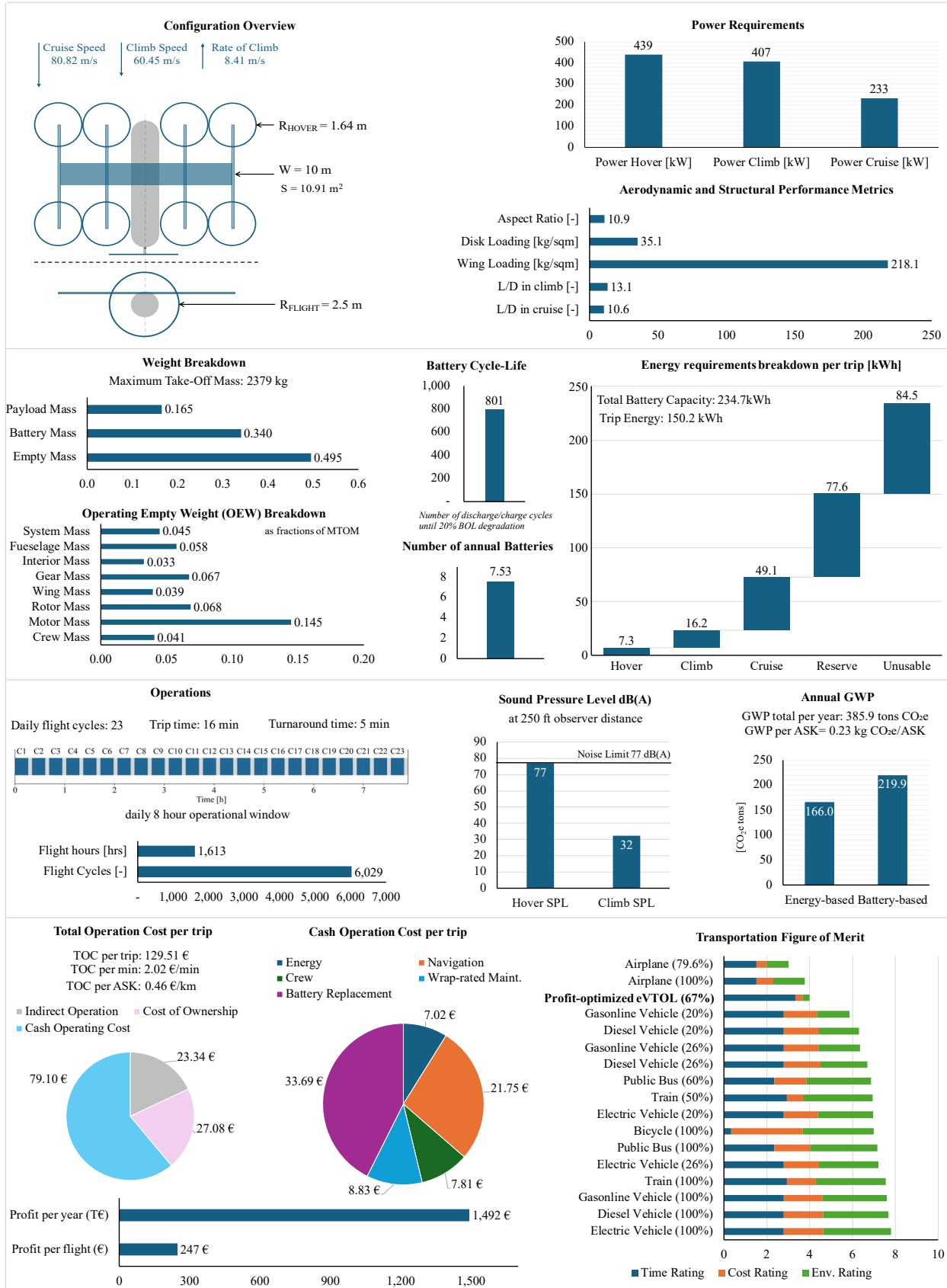


Figure 4: Optimization results of profit-maximizing conceptual eVTOL design: aircraft design, battery behavior, operating window usage, global warming potential, operating costs and cross-transportation comparison.

battery wear is used to compare eVTOL aircraft to existing means of transportation. In cross-transportation comparison, the design scores $R_{EVTOL_{time}} = 4.51$ for time but only $R_{EVTOL_{CO_2e}} = 1$ for emissions and $R_{EVTOL_{cost}} = 1$ for cost, yielding a composite FoM of 4. This places the eVTOL above only conventional aircraft and below gasoline internal combustion vehicles at 20% load factor, highlighting that although the design is highly profitable from the operator's point of view, it remains disadvantaged when compared to ground transport modes under equal weighting of time, cost, and environmental impact.

4.2 Cost-minimized eVTOL design

The TOC-minimizing eVTOL design, illustrated in Figure 5, was obtained after 9 iterations, 78 function evaluations, with a runtime of 1.17 seconds. The optimizer converged to a wingspan of 9.80 m with a chord of 1.0 m, a relatively small cruise propeller radius of 0.92 m, and hover rotors of 1.38 m, resulting in a maximum take-off mass of 1,633 kg. The empty-mass fraction is 0.51, with a battery fraction of 0.25, both in typical ranges for eVTOL aircraft [1]. At a pack-level energy density of 400 Wh/kg, the design requires 162 kWh of capacity, corresponding to a battery mass of 405 kg. Cruise speed is 71 m/s with a lift-to-drag ratio of 10.3, leading to a trip time of 18.1 minutes on the 70 km sizing mission. The configuration combines small-sized propeller radii and reduced mass fractions with a relatively low MTOM, reflecting the prioritization of cost reduction over utilization throughput and configuration complexity. Operationally, the charging rate is moderate at 1.9C, resulting in a turnaround time of 10.4 minutes and a block time of 28.5 minutes. This limits daily utilization to 17 flights and 4,379 annual cycles, equivalent to 1,324 annual flight hours. Profitability results from lower utilization offset by significantly reduced per-flight costs. Energy consumption per trip is 53.7 kWh. The depth-of-discharge of 0.33 together with an average discharge C-rate of 1.1 1/h extends the battery life to 2,015 cycles, resulting in 2.2 battery replacements per year and directly impacts recurring maintenance costs. The cost structure reflects these operational adjustments. Energy cost per trip is €5.20 (5.5% of TOC), annual salary-based crew cost is €10.76 (11% of TOC), and time-based maintenance is €9.98 (11% of TOC). Navigation charges, at €17.45 (18%), remain the highest single cost element, together with cost of ownership at €24.98 (26%), both scaling with MTOM. Battery-related costs are €9.24 per trip, corresponding to about 10% of total operating costs. Overall, total operating cost is minimized to €94.7 per flight, corresponding to €0.34 per seat-kilometer. Despite lower annual utilization, annual profit reaches €1.24 million, highlighting that cost savings can maintain economic viability even when throughput is reduced. SPL and environmental performance benefit from the MTOM and battery design, as the aircraft remains below the hover SPL limit at 74.9 dB(A). Annual operational GWP achieves 133 tons CO_{2e}, comparable to 31 gasoline-powered passenger vehicles or 117 electric-powered passenger vehicles driven for one year [79]. On a per-flight basis, emissions amount to 30 kg CO_{2e}, of which 67% are related to electricity generation and 33% to battery replacements. The limited number of battery replacements reduces the environmental burden of energy storage systems, making environmental performance more favorable. In cross-modal comparison, the TOC-minimized eVTOL achieves a balanced Figure of Merit. With a trip time of 18.1 minutes, it scores $R_{EVTOL_{time}} = 10$ for time. Cost performance remains low at $R_{EVTOL_{cost}} = 1.81$, while emissions performance reaches $R_{EVTOL_{CO_2e}} = 4.51$ due to limited battery turnover. The overall FoM is 5.44, placing this design closer to ground-based electric and diesel vehicles and well above conventional aviation, which indicates improved competitiveness in a broader transport context.

4.3 GWP-minimized eVTOL design

The GWP-minimizing eVTOL design, illustrated in Figure 6, was obtained after 6 iterations and 0.66 seconds of runtime. The optimization yields a wingspan of 15 m with a chord of 1.74 m, a cruise propeller radius of 1.59 m, and hover rotors of 1.56 m. This configuration results in a maximum take-off mass of 1,559 kg, with an empty-mass fraction of 0.54 and a battery fraction of 0.20. At a pack-level energy density of 400 Wh/kg, the design requires 127 kWh of capacity, corresponding to a battery mass of 318 kg. Cruise speed is computed as 43 m/s with a lift-to-drag ratio of 10, leading to a trip time of 29.4 minutes. The combination of large wing span and rotor radii with a relatively low MTOM reflects a prioritization of energy efficiency to minimize indirect operating emissions. The charging rate is set at 1C, resulting in an extended turnaround time of 24.4 minutes and a block time of 53.9 minutes per trip, constraining daily utilization to 8.9 flights and 2,317 annual cycles, equivalent to 1,136 flight hours. Energy demand per trip is 51.9 kWh, distributed across hover, climb, and cruise phases, with a depth-of-discharge of 0.41 and an average discharge C-rate of 0.83. These values indicate relatively gentle battery management, extending battery life substantially to approximately 5,723 charging cycles, resulting in fewer than one battery replacement per year. This very low replacement frequency directly reduces the emission burden associated with battery production and disposal, as well as battery-related replacement costs [28]. The cost structure is shaped by extended flight and turnaround times. Energy costs per trip are €5.02 (3.9% of TOC), navigation charges €16.98 (13% of TOC), and crew costs €20.34 (16% of TOC), becoming a dominant cost driver due to extended flight times. Time-based maintenance adds €16.18 per trip (12% of TOC). Battery-related costs are lowest with €2.56 per trip, representing 2% of total operating costs. Ownership costs are €45.50 per trip (35%), keeping total operating cost at €130 per flight, or €0.46 per seat-kilometer respectively. Despite the low frequency of operations, annual profit remains positive at €0.57 million. Noise and environmental performance benefit from

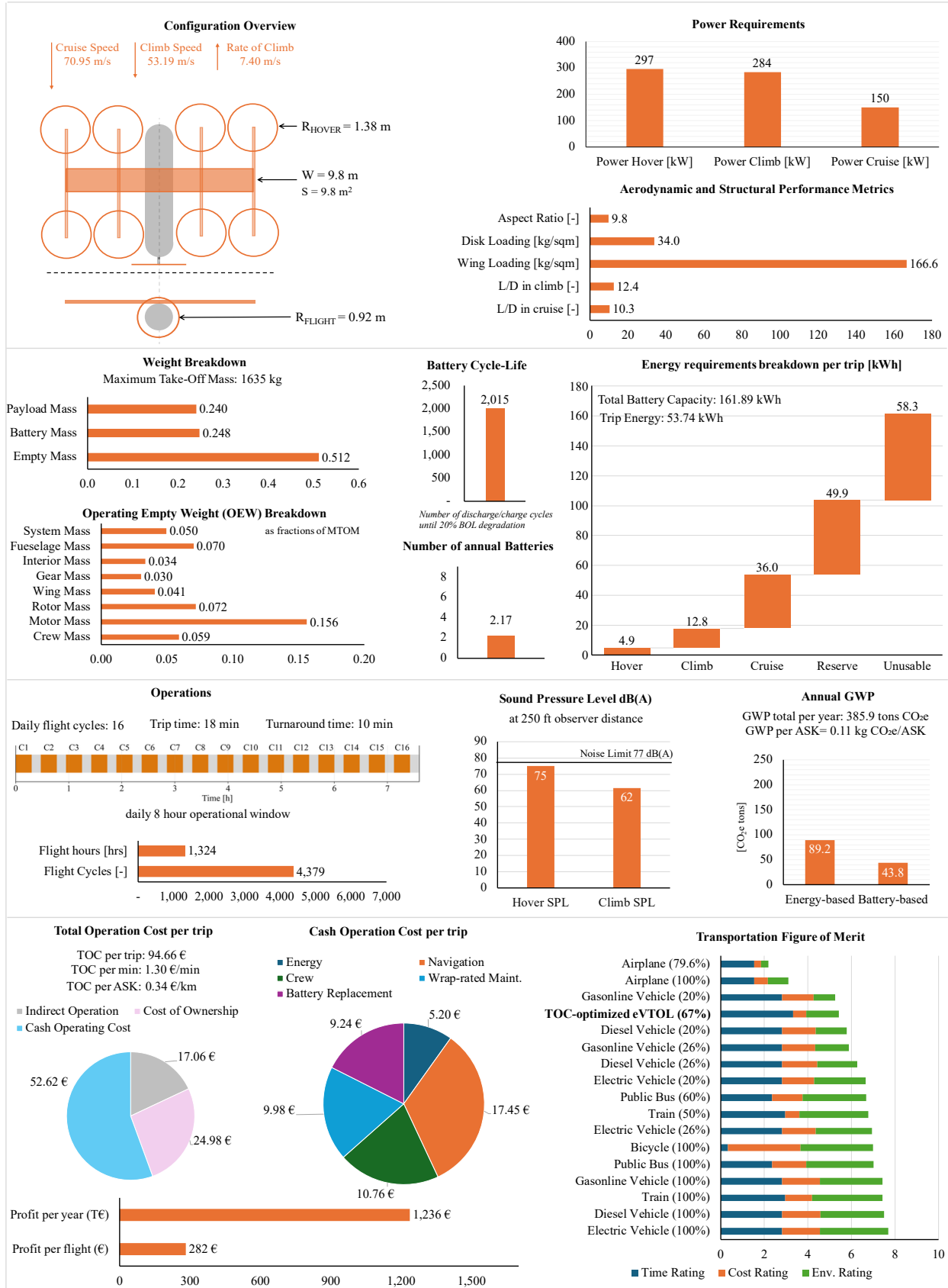


Figure 5: Optimization results of TOC-minimizing conceptual eVTOL design: aircraft design, battery behavior, operating window usage, global warming potential, operating costs and cross-transportation comparison.

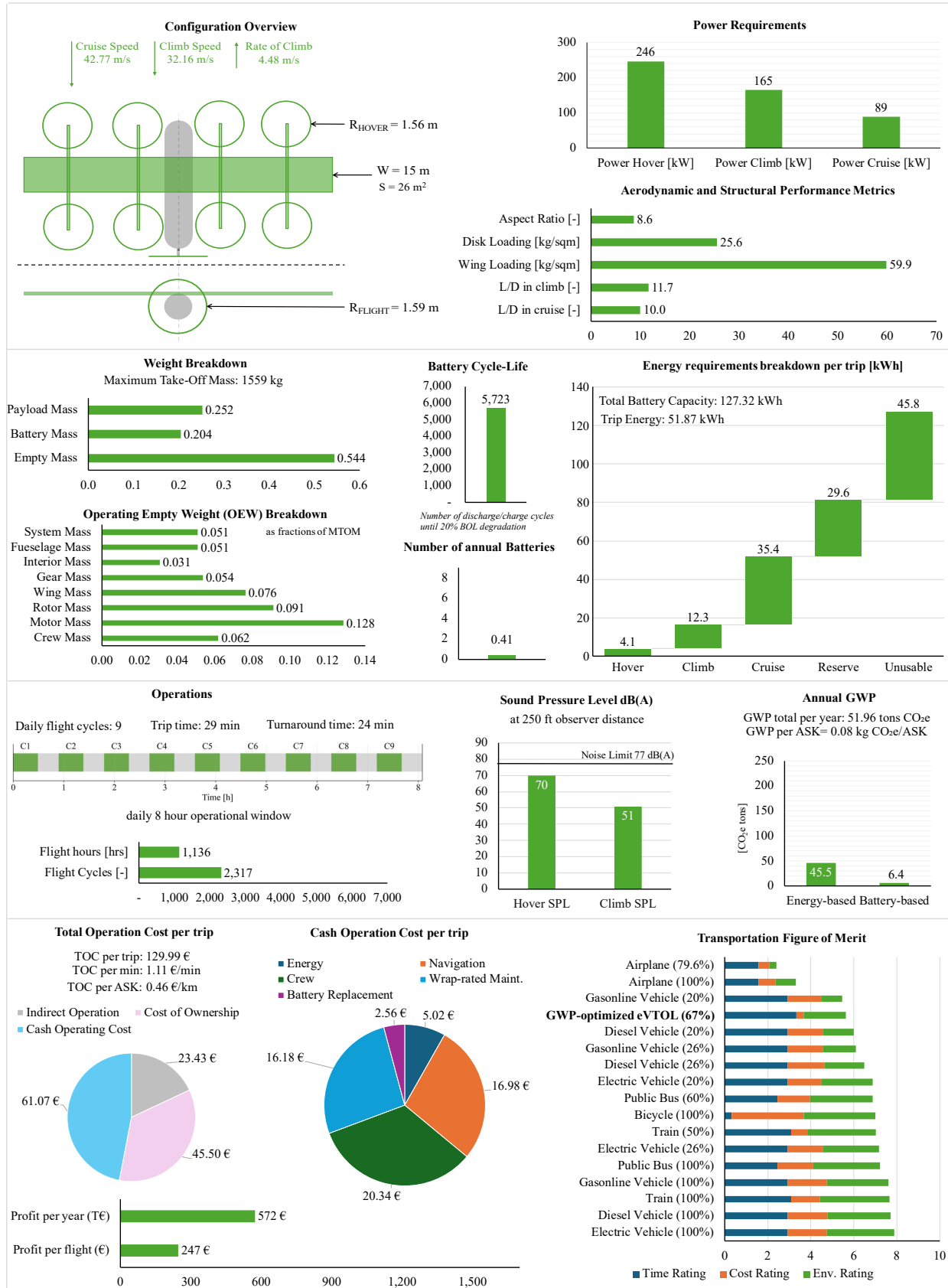


Figure 6: Optimization results of GWP-minimizing conceptual eVTOL design: aircraft design, battery behavior, operating window usage, global warming potential, operating costs and cross-transportation comparison.

the combination of moderate MTOM, large lifting surfaces, and gentle battery use. The design remains below the hover noise limit at 70 dB(A). Annual operational GWP is 51.96 tCO₂e, comparable to 12 gasoline-powered passenger vehicles or 46 electric-powered passenger vehicles driven for one year [79]. On a per-flight basis, emissions are 22.4 kg CO₂e, of which 88% are attributable to electricity generation and 12% to battery replacements. In cross-modal comparison, with a trip time of 29.4 minutes, this design scores $R_{EVTOL_{time}} = 10$ for travel time. Cost performance remains low at $R_{EVTOL_{cost}} = 1$, while emissions performance reaches $R_{EVTOL_{CO_2e}} = 5.95$ due to very low battery turnover and efficient flight. The overall FoM is 5.44, reflecting the design’s strong environmental profile in relation to its operational performance.

4.4 FoM-maximized eVTOL design

The FoM-maximizing eVTOL design, illustrated in Figure 7, converged after 4 iterations, 39 function evaluations, and 4 gradient evaluations, completing in 0.57 seconds. The optimizer yields a wing span of 14.65 m with a 1.0 m chord, a cruise propeller radius of 1.22 m, and hover rotors of 1.59 m. The resulting maximum take-off mass is 1,534 kg, with an empty-mass fraction of 0.54 and a battery fraction of 0.20. At a pack-level energy density of 400 Wh/kg, the required capacity of 122.53 kWh corresponds to a battery mass of 306 kg. Cruise is flown at 55 m/s with a lift-to-drag ratio of 11.4, giving a flight time of 23 minutes for the 70 km trip. The configuration represents a compromise, with a high aspect ratio wing and moderate rotor diameters, lower disk loading and power demand, while cruise speed remains high enough to ensure acceptable trip duration. Operational characteristics emphasize balance rather than extremes. Charging at 1.15C leads to a turnaround time of 19 minutes and a block time of 42 minutes per flight. This enables 11 flights per day, translating to 2,952 annual flight cycles, equivalent to 1,130 annual flight hours. Energy use per trip is 45.46 kWh, with a depth-of-discharge of 0.37 and an average discharge C-rate of 0.97 1/h. These values provide a battery life of 4,165 cycles, translating into 0.71 battery replacements per year, or one battery replacement every 1.41 years, respectively. The economic profile reflects this balance. Energy costs per trip are €4.39 (4% of TOC), crew costs €15.96 (15% of TOC), and navigation €16.82 (16% of TOC). Maintenance contributes €16.02 (15% of TOC), while cost of ownership accounts for €35.53 (34% of TOC), making it the highest cost component. Battery-related costs are minimal at €3.38 per trip (3% of TOC). The total operating cost is €108.22 per flight, or €0.39 per seat-kilometer. With ticket revenues assumed constant, profit amounts to €268 per flight, yielding €0.793 million annually. Environmental performance is shaped by low turnover of batteries and moderate energy demand. Each flight produces 20.89 kg CO₂e, dominated by electricity use, 82%, and 18% from battery replacement. On an annual basis, the design emits 61.68 tons CO₂e, comparable to 14 gasoline-powered passenger vehicles or 55 electric-powered passenger vehicles driven for one year [79]. The SPL remains within limits at 69 dB(A) during hover. In cross-modal comparison, the design achieves a moderate transportation Figure of Merit, ranking above gasoline-powered and diesel-powered passenger vehicles at 20% load factor, and right below the same at 26% load factor. With a trip time of 23.1 minutes, it scores $R_{EVTOL_{time}} = 10$ for time. Emissions performance reaches $R_{EVTOL_{CO_2e}} = 6.22$, while cost is rated at $R_{EVTOL_{cost}} = 1.29$. The overall FoM is 5.84, reflecting a configuration that balances energy efficiency, operating cost, and environmental performance.

5 Comparative assessment of optimized eVTOL designs

The analysis of four specialized eVTOL designs, optimized for maximum profit, minimum TOC, minimum GWP, and maximum FoM, highlights the trade-offs that arise when operational, economic, and environmental priorities are considered. Each configuration demonstrates specific advantages but also exposes limitations that may constrain its broader applicability. To assess conceptual alignment with UAM requirements, the designs are benchmarked against the Uber Elevate specifications [30, 53] in Table 5, focusing on key differences in performance and competitiveness. Finally, we discuss how these outcomes map to stakeholder priorities and their operational and regulatory implications.

Uber’s requirements emphasize motion efficiency and operational capability. The profit-optimized design, with its higher take-off mass (2,379 kg) and battery capacity (235 kWh), shows the lowest motion efficiency (0.96 km/kWh) and the highest power demands in both hover (439 kW) and cruise (233 kW) across the optimized eVTOL designs, deviating significantly from Uber’s target of 1.24 km/kWh. Additionally, this design has the shortest battery cycle life, leading to the highest battery and maintenance costs among all designs. It is evident that gentle charging strategies, such as those using a 1C rate within the GWP-, and FoM-optimized design, substantially increase battery cycle life. The TOC-, GWP-, and FoM-optimized designs align more closely with Uber’s baseline in terms of MTOM, deviating around 10%-15% from Uber’s requirements. The GWP-, and FoM-optimized designs achieve lower cruise power requirements than Uber’s target, albeit with a significant reduction in cruise speed. However, none of the designs meet the required 2,080 flight hours per year, with the profit-optimized design reaching only 1,613 hours, approximately 400 hours short of the target. This shortfall in flight hours, based on the slower cruise speed of the optimized eVTOL designs, could impact service availability and necessitate a larger fleet to meet demand, potentially driving up operational costs. Regarding costs per seat, which Uber sets at €19 for a typical trip, the TOC-optimized design achieves the lowest cost

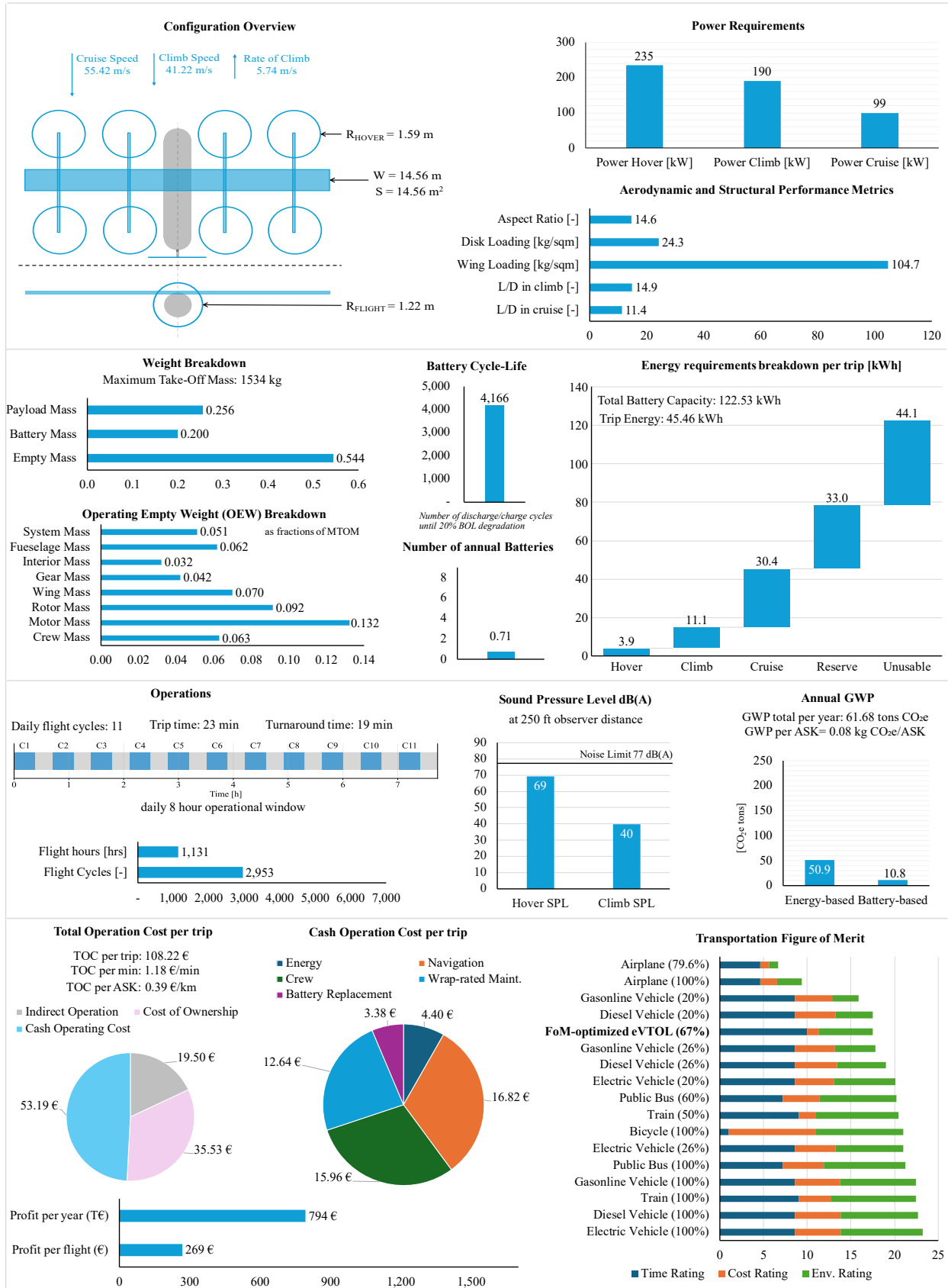


Figure 7: Optimization results of FoM-maximizing conceptual eVTOL design: aircraft design, battery behavior, operating window usage, global warming potential, operating costs and cross-transportation comparison.

	Uber Elevate [30]	Profit-opt.	TOC-opt.	GWP-opt.	FoM-opt.
Vehicle Design and Performance					
Maximum take-off mass [kg]	1,814	2,379	1,633	1,559	1,534
Battery specific energy [Wh/kg]	400	290	400	400	400
Battery cycle life [cycles]	2,000	801	2,015	5,723	4,166
Battery capacity [kWh]	140	235	162	127	123
Cruise speed [km/h]	320	291	255	154	200
Motion efficiency at cruise [km/kWh]	1.24	0.96	1.30	1.35	1.54
Power required at hover [kW]	500	439	297	246	235
Power required at cruise [kW]	120	233	150	89	99
Lift-to-drag ratio [-]	13	11	10	10	11
Economic Competitiveness					
Cost per pax-kilometer [€/km]	0.27	0.46	0.34	0.46	0.39
Cost per pax-minute travelled [€/min]	1.27	2.02	1.30	1.11	1.18
Cost of a 70 km pooled VTOL trip per person [€]	19	48	35	49	40
Vehicle utilization (hours per year)	2,080	1,613	1,324	1,136	1,131
Load factor (average seats filled)	67%	67%	67%	67%	67%
Operational Costs					
Piloting cost as % of direct operating costs	36%	7%	14%	19%	18%
Maintenance costs as % of direct operating costs	22%	40%	25%	18%	18%
Battery costs as % of direct operating costs	2%	32%	12%	2%	4%
Energy costs as % of direct operating costs	12%	7%	7%	5%	5%
Ownership costs as % of direct operating costs	8%	26%	32%	43%	40%

Table 5: Summary of Uber eVTOL UAM requirements and comparison with optimized designs.

among the specialized designs at €35. This indicates that further significant cost reductions are necessary to meet Uber's stringent economic goals. Potential cost savings are particularly apparent in ownership costs, which are tied to aircraft acquisition expenses. These costs are expected to decrease as production scales, potentially reducing overall operating costs in the long term. Additionally, improvements in battery technology, such as higher specific energy or faster charging methods beyond 1C, could further shift the economic balance, making these designs more viable. Overall, all designs fall within reasonable limits and are broadly aligned with Uber Elevate's requirements, suggesting potential real-world viability. The economic feasibility and operational implementation of these designs merit further research to ensure they can meet the demands of urban air mobility. Moreover, while the environmental benefits of the GWP-optimized design are clear, further assessment is needed to evaluate how these designs align with Uber's and the industry's broader sustainability strategy, particularly in terms of long-term environmental impact and scalability. This comparison illustrates that potential future large-scale UAM operators such as Uber are aiming for a hard balance in operational efficiency, such as high cruise speed at low power requirements combined with high demands in cost efficiency.

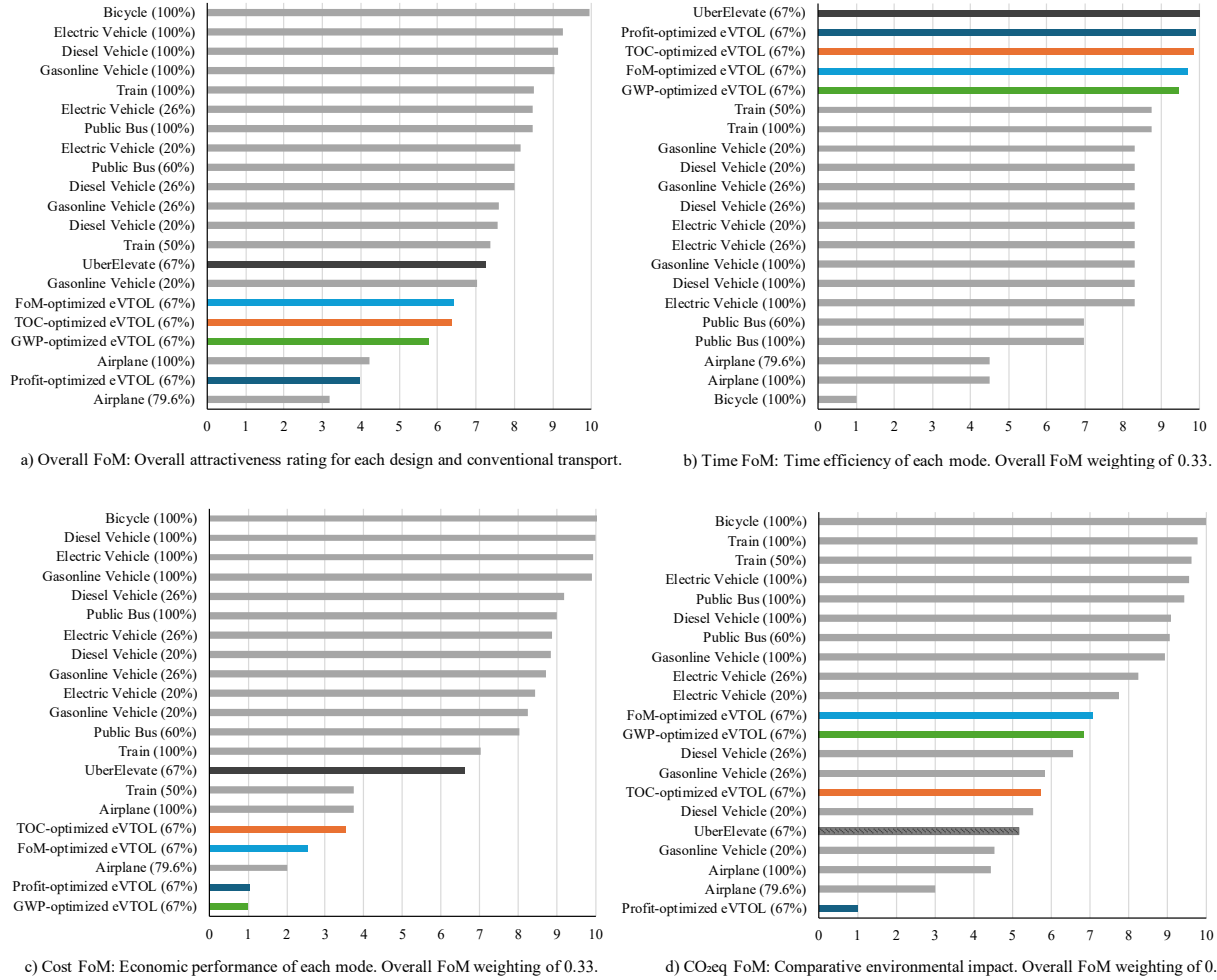


Figure 8: Comparative assessment of transportation Figure of Merit (FoM) for optimized eVTOL configurations and conventional transport modes as described in Section 3.1.7. The results, shown for the aggregated FoM (a) and its component dimensions of time (b), cost (c), and environmental impact (d), are benchmarked against industry-recognized UAM requirements derived from Uber Elevate requirements [53]. Source data for this comparison can be found in Table 5. The value presented for Uber Elevate in Figure (c) is a conceptual approximation based on the average of all eVTOL designs, as specific data for this metric was unavailable. It should be noted that this benchmarking serves to position the presented optimized designs against an established industry baseline and should not be taken as a formal evaluation of an Uber Elevate-specific design.

To understand the overall comparative viability of each design beyond these individual metrics, we introduce the Transportation Figure of Merit (FoM). As described in Section 3.1.7, the FoM addresses this by quantifying the total utility of each transport option, integrating time, cost, and environmental impact into a single rating. As depicted in Figure 8 (b), all eVTOL designs achieve the highest score for time efficiency, making them the superior choice for time-critical applications. In contrast, Figure 8 (c) reveals their significant comparative disadvantage in cost, where the profit-optimized design ranks lowest among all options, with even the TOC-optimized design placed in the lower quartile. Both perform significantly worse than fully-loaded ground-based transport modes like trains or electric passenger vehicles. The Uber Elevate benchmark, with its modest lead over trains in the cost category, indicates that cost is a critical lever for increasing the overall attractiveness and adoption of eVTOLs beyond niche markets.

Regarding environmental impact, Figure 8 (d) indicates that optimized eVTOLs perform moderately, except for the profit-maximized design, which scores poorly due to its high annual utilization of batteries and high energy demand. The Uber Elevate GWP rating is a conceptual approximation based on the average of the four optimized designs, as specific data were unavailable. The value is not intended as a formal evaluation of the Uber Elevate design. The environmental performance of any eVTOL is heavily dependent on the energy grid source and overall system efficiency.

The overall FoM in Figure 8 (a) reflects these trade-offs, showing that an objective, rationale-driven stakeholder who equally weights time, cost, and environmental impact would favor ground-based transport like electric cars or trains. This highlights that a straightforward equal weighting, while useful for a conceptual baseline comparison, may not fully capture the complexity of specific stakeholder preferences. For example, while the bicycle achieves the highest score, it is not a practical substitute for a 70 km eVTOL mission in a day-to-day transportation context. Future work should explore the use of variable weightings and vehicle load factors to reflect different stakeholder segments and incorporate additional metrics such as safety, acoustics, and last-mile accessibility to provide a more holistic, stakeholder-specific view.

Our findings on the high cost and environmental dependency of eVTOLs are consistent with the literature [25, 26, 27], as described in Section 2. However, the presented integrated MDO approach for the co-design of the eVTOL vehicle, with its conceptual operational, economic, and environmental outcomes, offers a unique systems-level insight into the comparative performance of a transport system based on stakeholder-specific design objectives. The presented cross-transportation FoM offers a generalizable framework to systematically benchmark eVTOLs against the broader transport system. Rather than converging to a single universal optimum, the demonstrated analysis highlights that eVTOL design outcomes are inherently contingent upon the weighting of economic, environmental, and operational objectives, thus underscoring the need for stakeholder-specific pathways in conceptual design.

6 Conclusion

Our multidisciplinary design optimization framework provides a platform for analyzing and optimizing technological, environmental, and economic interdependencies of the eVTOL ecosystem. The analysis of the specialized eVTOL designs provides important insights to address complex trade-offs between these domains, necessary to be considered by UAM stakeholders. Our results provide an in-depth assessment of four specialized eVTOL designs, each optimized for different objectives: maximum profit, minimum total cost of ownership (TOC), minimum global warming potential (GWP), and maximum figure of merit (FoM). The main conclusions from our work and UAM stakeholder strategies and recommendations are as follows:

A profit-optimized eVTOL design achieves substantial operational efficiency gains through short travel times and minimized turnaround and battery recovery times, yet its long-term sustainability is hindered by the environmental impact of current battery technologies, highlighting the need for advancements in battery recycling. In contrast, a TOC-optimized design maximizes cost efficiency but sacrifices operational flexibility and profitability, underscoring the importance of balancing cost minimization with operational performance metrics. A GWP-optimized design, while significantly reducing environmental impact, faces limitations in economic viability due to extended travel times and reduced flight cycles, as energy consumption-optimized airspeed and a battery charging management system tailored to longevity are decisive factors. Finally, a cross-transportational comparative FoM-maximized design provides a balanced design approach based on passenger preferences and comparability with ground transportation alternatives. This approach integrates cost efficiency, operational performance, and sustainability to provide a comprehensive solution for urban air mobility requirements.

Slow charging extends battery life and reduces the frequency of replacement, which reduces long-term costs and improves sustainability, as shown in the scenario for minimum GWP- and maximum FoM-eVTOL design. Despite increased turnaround times and potential losses in operational efficiency, the cost and ecological advantages outweigh the disadvantages. Battery swapping stations allow for quick replacement of discharged batteries at vertiports, reducing downtime and maximizing daily flight cycles. This increases profitability through more frequent flights, but comes with risks such as high investment costs, complex inventory management, and the need for standardized eVTOL designs. The regulatory and logistic challenges of integrating battery swapping and charging stations should be addressed in future work.

Removing vertiport dimension limitations allows for optimized eVTOL designs with larger wingspans and rotor diameters, improving aerodynamic efficiency, reducing energy consumption, and lowering costs. However, flight efficiency-optimized eVTOL designs are reaching the limits of existing helipads. Adaptive wing technologies, such as Airbus' Extra Performance Wing demonstrator [80], offer a solution by utilizing foldable and movable wings that both improve aerodynamics and ensure infrastructure compatibility. This innovation enables efficient use of existing landing sites, but increases technical complexity and requires careful consideration of certification.

In summary, a strategic focus on battery life extension, recycling processes, optimized vertiport utilization, and adaptive wing designs that combine efficient aerodynamic design with infrastructure compatibility is recommended. The further development of eVTOL technologies should be supported by life cycle analyses, precise noise modeling, and economic operational optimization. Future work should consider additional, critical multidisciplinary aspects like aeroelastic instabilities (important for higher aspect ratio wings) and thermal runaway phenomena (battery safety) to fully capture

the design complexity of future operational and regulatory frameworks. Close co-operation between industry and regulatory authorities is essential to make UAM sustainable and economically viable.

7 Supplementary Material

Supplementary material is available for download here: **Supplementary Material**.

The source code and industry design comparison file is available at: **GitHub**.

Funding Sources: This research did not receive any specific grant from funding agencies in the public, commercial, or not-for-profit sectors.

References

- [1] Lukas Kiesewetter, Kazi Hassan Shakib, Paramvir Singh, Mizanur Rahman, Bhupendra Khandelwal, Sudarshan Kumar, and Krishna Shah. A holistic review of the current state of research on aircraft design concepts and consideration for advanced air mobility applications. *Progress in Aerospace Sciences*, 142:100949, 2023.
- [2] A. W. Schäfer, S. R. H. Barrett, K. Doyme, L. M. Dray, A. R. Gnadt, R. Self, et al. *Technological, Economic and Environmental Prospects of All-electric Aircraft*. Springer Science and Business Media LLC, 2018.
- [3] European Union Aviation Safety Agency (EASA). Study on the societal acceptance of urban air mobility in europe. Available online: <https://www.easa.europa.eu/sites/default/files/dfu/uam-full-report.pdf>, May 2021. This study has been carried out for EASA by McKinsey & Company.
- [4] NASA Aeronautics Research Mission Directorate. Urban Air Mobility Reference Material. Available online: <https://sacd.larc.nasa.gov/uam-refs/>, 2024. Accessed: 2024-06-01.
- [5] DFS Deutsche Flugsicherung GmbH and SkyVector. Aviation navigation resources: Dfs aip and skyvector. Available online: DFS AIP (<https://aip.dfs.de/basicAIP/>), SkyVector (<https://skyvector.com>), 2024. Accessed: 2024-12-20.
- [6] Shugo Kaneko and Joaquim R.R.A. Martins. Simultaneous optimization of design and takeoff trajectory for an evtol aircraft. *Aerospace Science and Technology*, 155:109617, 2024.
- [7] D. Sarojini, M. L. Ruh, A. J. Joshy, J. Yan, A. K. Ivanov, L. Scotzniovsky, et al. *Large-Scale Multidisciplinary Design Optimization of an eVTOL Aircraft using Comprehensive Analysis*. American Institute of Aeronautics and Astronautics, 2023.
- [8] Joaquim R. R. A. Martins and Andrew Ning. *Engineering Design Optimization*. Cambridge University Press, 2021.
- [9] M. L. Ruh, A. Fletcher, D. Sarojini, M. Sperry, J. Yan, L. Scotzniovsky, et al. *Large-scale Multidisciplinary Design Optimization of a NASA Air Taxi Concept using a Comprehensive Physics-based System Model*. American Institute of Aeronautics and Astronautics, 2024.
- [10] D. Keijzer, C. Simon Soria, J. Arends, B. Sarigol, F. Scarano, and S. G. Castro. *Design of a Hydrogen-Powered Crashworthy eVTOL Using Multidisciplinary Analysis and Design Optimization*. American Institute of Aeronautics and Astronautics, 2024.
- [11] T. H. Ha, K. Lee, and J. T. Hwang. Large-scale design-economics optimization of evtol concepts for urban air mobility, 2019. 10.2514/6.2019-1218.
- [12] P. K. Chinthoju, Y. H. Lee, G. K. Das, K. A. James, and J. T. Allison. *Optimal Design of eVTOLs for Urban Mobility using Analytical Target Cascading (ATC)*. American Institute of Aeronautics and Astronautics, 2024.
- [13] A. Brown and W. L. Harris. A vehicle design and optimization model for on-demand aviation. *AIAA/ASCE/AHS/ASC Structures, Structural Dynamics, and Materials Conference*, 2018.
- [14] Michael D. Patterson, Kevin R. Antcliff, and Lee W. Kohlman. A proposed approach to studying urban air mobility missions including an initial exploration of mission requirements. Available online: <https://ntrs.nasa.gov/api/citations/20190000991/downloads/20190000991.pdf>, 2018.
- [15] Christopher Silva, Wayne Johnson, Ken Antcliff, and Michael D. Patterson. Vtol urban air mobility concept vehicles for technology development, 2018.
- [16] Chi Yang, Yuchen Gao, Weigang Wei, Chang Liu, Kai Wang, Yue Zhang, Haiping Liu, Xiaoqing Lu, Fei Ren, Yuyi Yang, Kejie Li, and Xinfeng Zhao. Challenges and key requirements of batteries for electric vertical takeoff and landing aircraft. *Joule*, 5(8):1884–1900, 2021. Accessed: 2024-06-12.
- [17] Aishwarya Kasliwal, Nicholas J. Furbush, John H. Gawron, James R. McBride, Timothy J. Wallington, Robert D. De Kleine, et al. *Role of Flying Cars in Sustainable Mobility*. Springer Science and Business Media LLC, 2019.
- [18] N. André and M. Hajek. *Robust Environmental Life Cycle Assessment of Electric VTOL Concepts for Urban Air Mobility*. American Institute of Aeronautics and Astronautics, 2019.
- [19] Y. Mihara, P. Pawnlada, A. Nakamoto, T. Nakamura, M. Nakano, and P. Pawnlanda. Cost analysis of evtol configuration design for an air ambulance system in japan. *Journal of Advanced Transportation*, 2021:Article ID 8821234, 2021. Available online.
- [20] Y. Liu and C. Gao. *Assessing Electric Vertical Take-Off and Landing for Urban Air Taxi Services: Key Parameters and Future Transportation Impact*. MDPI AG, 2024.

- [21] Anna Straubinger and Julia Schaumeier. A critical perspective on the sustainability of urban air mobility. ZEW – Leibniz Centre for European Economic Research and Bauhaus Luftfahrt e.V., 2023.
- [22] Anna Straubinger, Erik T. Verhoef, and Henri L.F. de Groot. Going electric: Environmental and welfare impacts of urban ground and air transport. *Transportation Research Part D: Transport and Environment*, 102, 103146, 2022.
- [23] Khashayar Khavarian and Kara M. Kockelman. Life-cycle analysis of electric vertical take-off and landing vehicles. *Transportation Planning and Technology*, 47(8), 1227–1242, 2024. Published online: 01 Jun 2023.
- [24] Marco Fioriti, Marco Borghi, and Guido Pavan. Environmental and economic assessment of an evtol aircraft fleet for urban air mobility. 34th Congress of the International Council of the Aeronautical Sciences (ICAS), Florence, Italy, September 9–13, 2024.
- [25] Nabil Hagag and Bastian Hoeveler. The feasibility of electric air taxis: Balancing time savings and co2 emissions – a joint case study of respective plans in paris. Research Report, DLR Institute of Flight Guidance and Axalp Technologies AG, 2023. Case study of eVTOL operations in Paris during the 2024 Olympic Games.
- [26] Daniel Perez, Heeseung Shon, Bo Zou, and Kenneth Kuhn. Advanced air mobility for commuting? an exploration of economic, energy, and environmental feasibility. *Transport Economics and Management*, Vol. 3, pp. 135–152, 2025.
- [27] Teresa Donateo and Antonio Ficarella. A methodology for the comparative analysis of hybrid electric and all-electric power systems for urban air mobility. *Energies*, Vol. 15, No. 2, Article 638, 2022.
- [28] F. Arshad, J. Lin, N. Manurkar, E. Fan, A. Ahmad, M. Tariq, et al. Life cycle assessment of lithium-ion batteries: A critical review. *Resources, Conservation and Recycling*, 180, 2022.
- [29] H. B. Faulkner. The ata-67 formula for direct operating cost. Available online: <https://ntrs.nasa.gov/api/citations/19730024119/downloads/19730024119.pdf>, May 1973.
- [30] Jeff Holden and Nikhil Goel. Fast-forwarding to a future of on-demand urban air transportation. Available online: https://evtol.news/_media/PDFs/UberElevateWhitePaperOct2016.pdf, 2016.
- [31] Nicolas André and Manfred Hajek. Robust environmental life cycle assessment of electric vtol concepts for urban air mobility. AIAA Aviation 2019 Forum, Dallas, Texas, 17–21 June, 2019.
- [32] G. Gabrielli and T. von Kármán. What price speed? specific power required for propulsion of vehicles. Reprinted from *Mechanical Engineering*, Vol. 72, No. 10, 1950. Thurston Lecture.
- [33] Janet Yong, Rod Smith, Linda Hatano, and Stuart Hillmansen. What price speed – revisited. *Ingenia*, Issue 22, pp. 46–51, 2005. Railway Research Group, Imperial College London.
- [34] Dinda Andiani Putri, Johannes Frank, Maximilian Schopp, and Dieter Scholz. Comparing modes of transportation with an improved karman-gabrielli diagram. Poster, Hamburg University of Applied Sciences, Department of Automotive and Aeronautical Engineering, 2023. Bachelor Thesis and Poster Presentation, HAW Hamburg.
- [35] Patrick Moriarty and Stephen Jia Wang. Eco-efficiency indicators for urban transport. *Journal of Sustainable Development of Energy, Water and Environment Systems*, Vol. 3, No. 2, pp. 183–195, 2015.
- [36] Sheila Serafim da Silva, Ilton Curty Leal Junior, and Vanessa de Almeida Guimarães. Modal choice method to passenger transportation based on eco-efficiency measures. Conference Paper, XI Congreso de Ingeniería del Transporte (CIT 2014), Procedia – Social and Behavioral Sciences, 2014. Available at <https://www.researchgate.net/publication/338429278>.
- [37] A. B. Lambe and J. R. A. Martins. Extensions to the design structure matrix for the description of multidisciplinary design, analysis, and optimization processes. *Structural and Multidisciplinary Optimization*, 46(2):273–284, 2012.
- [38] Fuelbirds. Helicopter pads and helipads: How to select the right one for your needs. Available online: <https://www.fuelbirds.com/helicopter-pads-and-helipads-how-to-select-the-right-one-for-your-needs/>, 2023. Accessed: 2024-07-17.
- [39] European Union Aviation Safety Agency (EASA). Special condition for small-category vtol-capable aircraft, issue 2. Available online: <https://www.easa.europa.eu/sites/default/files/dfu/sc-vtol-issue-2.pdf>, June 2024. Accessed: 2024-06-10.
- [40] European Union Aviation Safety Agency. Special condition vtol. Available online: <https://www.easa.europa.eu/en/document-library/product-certification-consultations/special-condition-vtol>, 2024. Accessed: 2024-06-12.
- [41] Daniel P. Raymer. *Aircraft Design: A Conceptual Approach*. AIAA Education Series. American Institute of Aeronautics and Astronautics, 2nd edition, 1992.

- [42] Snorri Gudmundsson. *General Aviation Aircraft Design: Applied Methods and Procedures*. Butterworth-Heinemann, 2013. Accessed: 2024-08-08.
- [43] European Union Aviation Safety Agency. EASA review of standard passenger weights 2022 shows no significant change. Available online: <https://www.easa.europa.eu/en/newsroom-and-events/news/easa-review-standard-passenger-weights-2022-shows-no-significant-change>, 2022. Accessed: 2024-06-12.
- [44] B. Govindarajan and A. Sridharan. Conceptual sizing of vertical lift package delivery platforms. *Journal of Aircraft*, 57(6):1170, 2020.
- [45] S. S. Chauhan and J. R. R. A. Martins. Tilt-wing evtol takeoff trajectory optimization. *Journal of Aircraft*, 57(1):93, 2019.
- [46] Mark Drela. Xfoil: An analysis and design system for low reynolds number airfoils, 1989.
- [47] Constantin Rotaru and Michael Todorov. *Helicopter Flight Physics*. IntechOpen, February 2018. Licensed under CC BY 4.0.
- [48] James F. Marchman III. *Altitude Change: Climb and Glide*, chapter 5. James F. Marchman III in association with the University Libraries at Virginia Tech, 2021.
- [49] Matthew B. Galles. Reducing the Noise Impact of Unmanned Aerial Vehicles by Flight Control System Augmentation. Available online: <https://ntrs.nasa.gov/citations/20205004236>, August 2019.
- [50] Arthur F. Deming. Propeller Rotation Noise due Torque and Thrust. Available online: <https://ntrs.nasa.gov/citations/19930081525>, 1940.
- [51] L. Guting. On the Sound Field of Rotating Propeller. Available online: <https://ntrs.nasa.gov/citations/20030068996>, 1948.
- [52] R. Schlegel and R. King and H. Mull. Helicopter Rotor Noise Generation and Propagation. Available online: <https://apps.dtic.mil/sti/tr/pdf/AD0645884.pdf>, October 1966.
- [53] Uber Elevate. Summary of mission and requirements for uberair vehicles. Available online: <https://s3.amazonaws.com/uber-static/elevate/Summary+Mission+and+Requirements.pdf>, December 2023. Accessed: 2024-06-23.
- [54] International Civil Aviation Organization (ICAO). Airlines operating costs and productivity. Available online: <https://www.icao.int/mid/documents/2017/aviation%20data%20and%20analysis%20seminar/ppt3%20-%20airlines%20operating%20costs%20and%20productivity.pdf>, 2017. Accessed: 2024-06-16.
- [55] Investopedia. Annuity method of depreciation. [https://www.investopedia.com/terms/a/annuity-method-of-depreciation.asp#:~:text=The%20annuity%20method%20of%20depreciation%20is%20a%20process%20used%20to,least%20constant\)%20rate%20of%20return.](https://www.investopedia.com/terms/a/annuity-method-of-depreciation.asp#:~:text=The%20annuity%20method%20of%20depreciation%20is%20a%20process%20used%20to,least%20constant)%20rate%20of%20return.), 2023. Accessed: 2024-06-15.
- [56] Taxi fare calculator london. <https://www.bettertaxi.com/taxi-fare-calculator/london/>. Accessed: 2024-08-19.
- [57] International Energy Agency (IEA). Germany - countries & regions. <https://www.iea.org/countries/germany>, 2024. Accessed: 2024-08-29.
- [58] IPCC. Annex iii: Technology-specific cost and performance parameters. https://www.ipcc.ch/site/assets/uploads/2018/02/ipcc_wg3_ar5_annex-iii.pdf, 2014. Accessed: 2024-08-29.
- [59] World Nuclear Association. Carbon dioxide emissions from electricity, 2024. Accessed: 2024-08-29.
- [60] ADAC. Vw golf – modelle und technische daten. <https://www.adac.de/rund-ums-fahrzeug/autokatalog/marken-modelle/vw/vw-golf/>, 2025. Accessed: 2025-08-28.
- [61] Statista. Average price of super e10 fuel in germany from january 2021 to august 2025. <https://www.statista.com/statistics/1292467/super-10-fuel-average-price-germany/>, 2025. Accessed: 2025-08-28.
- [62] Comcar. Co2 emissions per litre of fuel. <https://comcar.co.uk/emissions/co2litre/>, 2025. Accessed: 2025-08-28.
- [63] ADAC. Vw golf – models and technical data. <https://www.adac.de/rund-ums-fahrzeug/autokatalog/marken-modelle/vw/vw-golf/>, 2025. Accessed: 2025-08-28.
- [64] Cambridge Regional College. How much energy do you use? https://www.sustainabilityexchange.ac.uk/files/cambridge_regional_college_sus_how_much_energy_do_you_use.pdf, 2025. Accessed: 2025-08-28.

- [65] Statista. Average price of diesel fuel in germany from january 2021 to august 2025. <https://www.statista.com/statistics/1330032/diesel-average-price-germany/>, 2025. Accessed: 2025-08-28.
- [66] Michelin Connected Fleet. How to calculate co2 emissions of your fleet. <https://connectedfleet.michelin.com/blog/calculate-co2-emissions/#:~:text=0ne%20litre%20of%20diesel%20creates,has%20emitted%20in%20a%20month.>, 2025. Accessed: 2025-08-28.
- [67] EV Database. Tesla model y long range dual motor. <https://ev-database.org/uk/car/1619/Tesla-Model-Y-Long-Range-Dual-Motor>, 2025. Accessed: 2025-08-28.
- [68] Statista. Electricity prices for charging stations for electric cars in germany in 2024, by provider. <https://www.statista.com/statistics/1167538/electricity-prices-charging-stations-electric-cars-by-provider-germany/>, 2025. Accessed: 2025-08-28.
- [69] H. van Essen, A. Schrotten, M. Otten, D. Sutter, C. Schreyer, R. Zandonella, M. Maibach, and C. Dolan. External costs of transport in europe. <https://www.sciencedirect.com/science/article/pii/S0965856415001354>, 2015. Accessed: 2025-08-28.
- [70] FlixBus and Atmosfair. Well-to-wheel analysis. <https://cdn-cf.cms.flixbus.com/drupal-assets/2023-05/Well-to-Wheel%20Analysis%20atmosfair.pdf>, 2023. Accessed: 2025-08-28.
- [71] ChemEurope. Fuel efficiency in transportation. https://www.chemeuropa.com/en/encyclopedia/Fuel_efficiency_in_transportation.html, 2025. Accessed: 2025-08-28.
- [72] Siemens Mobility. Ice 4 high-speed and intercity train. <https://www.mobility.siemens.com/global/en/portfolio/rolling-stock/high-speed-and-intercity-trains/ice-4.html>, 2025. Accessed: 2025-08-28.
- [73] Skytanking. Jet fuel – glossary entry. <https://www.skytanking.com/news-info/glossary/jet-fuel/>, 2025. Accessed: 2025-08-28.
- [74] International Air Transport Association (IATA). Iata carbon offset program – frequently asked questions. https://www.iata.org/contentassets/922ebc4cbcd24c4d9fd55933e7070947/icop_faq_general-for-airline-participants.pdf, 2021. Accessed: 2025-08-28.
- [75] Sustrans. Can we put a figure on the value of cycling to society? <https://www.sustrans.org.uk/our-blog/opinion/2016/march/can-we-put-a-figure-on-the-value-of-cycling-to-society>, 2019. Accessed: 2025-08-28.
- [76] M. Lenzen. Total requirements of energy and greenhouse gases for australian transport. <https://www.sciencedirect.com/science/article/pii/S1361920999000097>, 1999. Accessed: 2025-08-28.
- [77] Patrick Wills. Expert interview/correspondence with helipaddy limited founder. Email, 2024. Average existing helipad dimension for UAM can be assumed to be 15m.
- [78] Federal Aviation Administration (FAA). Integration of powered-lift: Pilot certification and operations; miscellaneous amendments related to rotorcraft and airplanes – final rule. Available online: <https://www.faa.gov/newsroom/integration-powered-lift-pilot-certification-and-operations-miscellaneous-amendments>, July 2024. Final rule amending pilot certification and operational requirements for powered-lift aircraft.
- [79] U.S. Environmental Protection Agency. Greenhouse gas equivalencies calculator, 2025. Last updated February 24, 2025.
- [80] Airbus. Extra performance wing demonstrator takes off. Available online: <https://www.airbus.com/en/newsroom/stories/2023-11-extra-performance-wing-demonstrator-takes-off>, 2023. Accessed: 2023-11-12.